CRYO/00/017
October 7, 2000

Thermal, Hydraulic and Electric Analysis of Superconducting Cables: Model Description

L. Bottura, C. Rosso

Distribution: restricted

Summary

This note describes a generic, multi-component and multi-channel model for general, consistent and simultaneous analysis of thermal, electric and hydraulic transients in superconducting cables. The model is devised for most general situations, but reduces in limiting cases to commonly known models without loss of efficiency. In the note we give details on the governing equations and describe the solution method used to deal with the high numerical complexity of the coupled field problem.

1 Background

The transient behavior of superconducting cables is determined by intrinsically coupled thermal, hydraulic and electric phenomena. The coupling among the three fields makes analytical treatment of transient response of superconductors exceedingly difficult. This is in particular true in kA-class, low-Tc superconducting cables, where the coupling among the thermal, hydraulic and electric phenomena takes place on comparable time scales [1]. On the other hand understanding of the coupled behavior is presently recognized as extremely important to guarantee optimal design at proper operating margin. Furthermore new applications of high-Tc materials, e.g. power transmission cables, call for an effort similar to the one already performed for low-Tc material to understand and control thermal and electric performance. Present models for thermal, hydraulic or electric analysis of cables are not consistent as they generally lack proper coupling. In addition they have a specific and restricted field of application, and are difficult to extend parametrically to different cable geometries or operating conditions.

This note describes the general model that we have developed for consistent and easy parametric analysis of superconducting cables. The model can be used for a large variety of cable configurations and operating conditions. As *model* we define the set of Partial Differential Equations (PDE's) that describe the evolution of the state variables of the coupled system. In the following sections we present the concept of the model and the equations forming the system of

PDE's, detailing their derivation. We put then the system of equations in a form suitable to numerical treatment, and we finally describe the solution strategy which is based on a finite element discretization in space and finite differences in time.

2 Model Generalities

To derive the model for the coupled analysis of thermal, hydraulic and electric transients we ideally subdivide a superconducting cable in an assembly of components. Components can be of *thermal*, *hydraulic* or *electric* nature. Thermal components are all the solid cable components, structures, electrical barriers where the state is described by the temperature field. Hydraulic components are the cooling channels in a cable, whose state is described by the flow velocity and by the temperature and pressure of the coolant. Electric components are all current carrying elements, either super- or normal-conducting, whose state is defined by the current field. Thermal and electric domains can *overlap*, i.e. the same physical entity (e.g. a superconducting strand) can be modelled both as a thermal and an electric component.

We make the assumption that a superconducting cable has a large ratio of length to cross sectional dimension, so that all components can be considered as 1-D with good approximation. This is equivalent to saying that the state of each component is uniform in the two dimensions in the cable cross section, and can only change along the cable.

An example of subdivision of a cable in a set of components is given in Fig.1 for a fusion cable-in-conduit conductor. We have identified as thermal components the cable bundle and the jacket. The hydraulic components are the interstitial helium flow in the cable sub-units and the central cooling channel. No electric components have been used, assuming a uniform currnt distribution within the cable. This subdivision results in a model that is identical to the one described in [8]. In Fig. 2 we show an analogous subdivision for an accelerator Rutherford cable. In this case the thermal and electric components are coincident with the single strands, while the hydraulic component is a single and large channel that models the helium bath in which the cable operates.

Both examples above are arbitrary, but are suited to illustrate the meaning of the subdivision process. In addition they suggest that it is possible to take into account gradients in the cable cross section by subdividing the cable in an appropriate number of independent components. Therefore, although the model is based on a 1-D assumption, the 3-D temperature, flow and current fields in the cable can be topologically described by the equivalence with the assembly of all components.

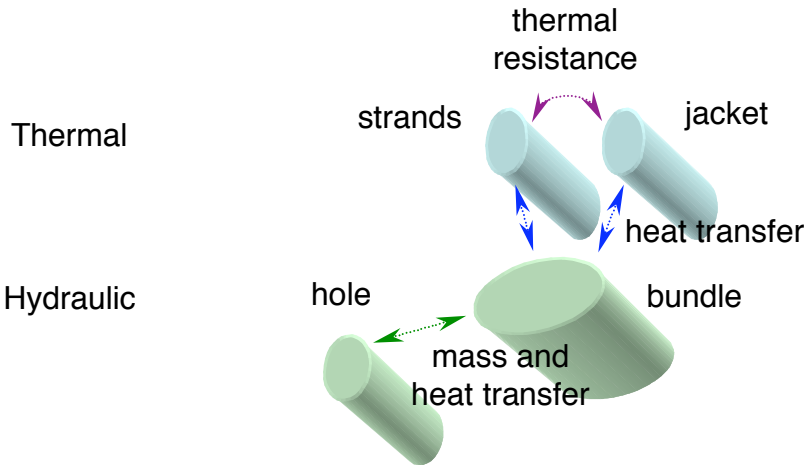

Figure 1. Cable-in-conduit conductor with central cooling hole for fusion applications and its schematic representation in term of thermal and hydraulic components. No electric component has been considered in this representation. The strands in he cable are assumed at uniform temperature and uniform current distribution, and are coupled to the jacket through thermal resistance. Two cooling channels are modelled separately, coupled among themselves through mass and heat transfer. Heat transfer couples the strand and the jacket to the helium in the cable bundle.

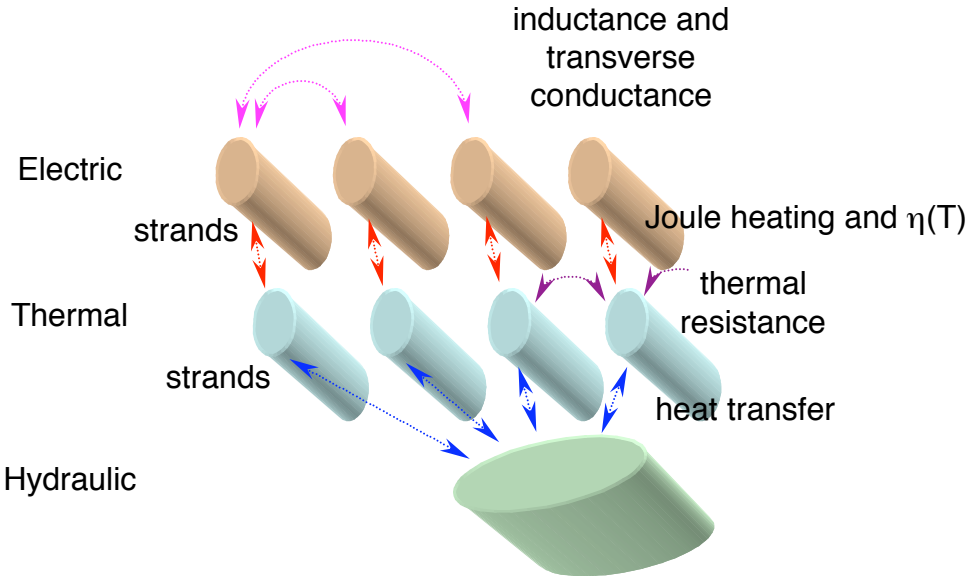

Figure 2. Accelerator Rutherford cable and its schematic representation in term of thermal, hydraulic and electric components. Single strands are modelled using both thermal and electric components coupled through current dependent heating and temperature dependent resistance. For simplicity only 4 electric and thermal components are shown. The electric components are coupled among themselves through inductance and transverse conductance, while the thermal components are components are coupled through heat resistances. All thermal components in addition are coupled to a single hydraulic components modelling a helium bath through heat transfer.

Once the subdivision process has taken place, our approach is to define the partial differential equations that govern the evolution of the state variables for each component in the cable. In the *thermal* components the temperature field is described by a set of diffusion equations. For the *hydraulic* components the flow velocity, pressure and temperature are described by mass, momentum and energy conservation balances. Finally the current behaviour in the set of *electric* components is described by a set of semi-continuum circuital equations.

One independent PDE is written for each state variable in a component. The assembly of all PDE's gives the system to be integrated in time and space starting from a given initial condition and with a given set of boundary conditions. The components are *coupled* to take in proper account the interaction among the temperature, flow and current fields. The coupling can take place among components of the same type (e.g. thermal coupling among the thermal components, inductive coupling among the electric components) as well as among components of different type (e.g. heat exchange between thermal and hydraulic components). Coupling is either explicit, through relations among the state variables, or implicit, through the dependence of the material properties in a domain on the value of the state variables of other domains.

3 Thermal Components

The thermal components of a superconducting cable can be of various nature: superconducting strands, structural components, electrical barriers, insulators and others. All these material can generate Joule heat, transport heat by conduction, and exchange heat at their mutual interface and at the interface with a cooling medium. Assuming that the transverse dimension of each component is small with respect to its length we can write a general 1-D heat transport equation for each component i:

$$A_i \rho_i C_i \frac{\partial T_i}{\partial t} - \frac{\partial}{\partial x}\left(A_i k_i \frac{\partial T_i}{\partial x} \right) = \dot{q}'_i + \dot{q}'_{Joule,i} + \dot{q}'_{transverse,i} + \sum_{\substack{j=1 \\ j \neq i}}^{N} \frac{\left(T_j - T_i\right)}{H_{ij}} + \sum_{h=1}^{H} p_{ih} h_{ih} \left(T_h - T_i\right) \qquad (3.1)$$

where A_i is the cross section of the component, in principle a function of position, ρ_i its density, C_i the specific heat, k_i the thermal conductivity and T_i the temperature. The total number of components is N. We allow each component to have an internal structure, assuming that the temperature within the cross section of the component is constant. This is for instance the case of a superconducting strand composed of superconducting filaments embedded in a stabilizer matrix. A schematic representation of a component with an internal structure is given in Fig. 3.

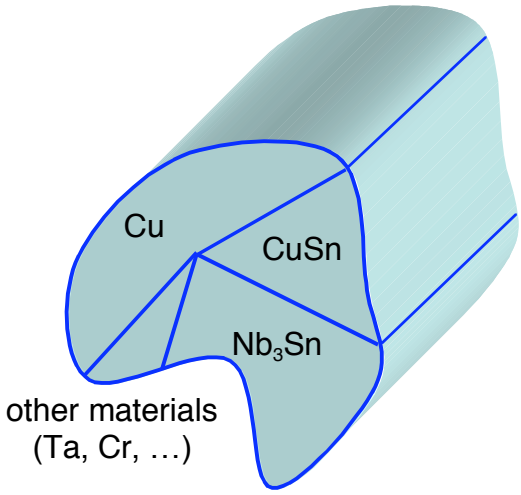

Figure 3. Schematic representation of a thermal component with several materials forming its internal structure. In the picture a Nb_3Sn single strand is ideally subdivided in its single materials (Nb_3Sn, copper, bronze, traces of other materials). The materials in the component have the same temperature. For the subdivision the shape of the cross section is not important, only the relative composition is of relevance in the calculation of the homogeneised properties.

For each component the homogenised characteristics, used in Eq. (3.1), are defined based on the following rules:

$$A_i = \sum_{m=1}^{M_i^m} A_i^m \tag{3.2}$$

$$\rho_i = \frac{\sum_{m=1}^{M_i^m} \rho_i^m A_i^m}{A_i} \tag{3.3}$$

$$C_i = \frac{\sum_{m=1}^{M_i^m} \rho_i^m A_i^m C_i^m}{A_i \rho_i} \tag{3.4}$$

$$K_i = \frac{\sum_{m=1}^{M_i^m} K_i^m A_i^m}{A_i} \tag{3.5}$$

where M_i^m is the number of different materials within the component i , and superscript m indicates the characteristics of each material. In addition to the rules above, it is useful to introduce here the rule for the homogeneisation of the electrical resistivity η_i, to be used later in the calculation of the Joule heating:

$$\frac{1}{\eta_i} = \frac{\sum_{m=1}^{M_i^m} \frac{1}{\eta_i^m} A_i^m}{A_i} \tag{3.6}$$

Heat is either generated by an external source $\dot{q}_i'$, it is due to the Joule heat $\dot{q}'_{Joule,i}$ if the component is carrying a current, is generated by the current circulating among components through the transverse electrical resistance $\dot{q}'_{transverse,i}$, or is exchanged with other thermal components or coolants as modeled by the last two sums in Eq. (2.1). In the case of heat exchange among components we have introduced the thermal resistance per unit length H_{ij} between components i and j (this last at temperature T_j). The heat exchanged with H different coolant channels depends on the wetted perimeter p_{ih} and heat transfer coefficient h_{ih} with the coolant flowing in channel h at temperature T_h. We will discuss the details of the heat transfer coefficient when dealing with the model for the hydraulic components.

3.1 Joule Heat

The Joule heat term depends on the current carried by the cable component I_i and on the electric field E_i developed along its length. In general terms we can write that:

$$\dot{q}'_{Joule,i} = I_i E_i \tag{3.7}$$

where, for consistency with the 1-D approximation made so far, we have assumed that current and electric field have the same direction. Note that this assumption is no longer exact if the current redistributes along the length of the cable. In this case additional heat is generated in the transverse resistance, as will be discussed later dealing with the coupling of the thermal and electric models.

In the case of a purely resistive material there is a linear relation between the electric field and current density in the material:

$$E_i = \eta_i J_i \tag{3.8}$$

where η_i is the average electrical resistivity of the component and J_i the current density defined as:

$$J_i = \frac{I_i}{A_i} \tag{3.9}$$

For a component containing a superconducting material in parallel with a stabilizing shunt the relation is more complex. The electric field in a superconducting strand or cable is obtained experimentally and is usually fitted using a power law:

$$E_i = E_0 \left(\frac{I_i}{I_c} \right)^n \tag{3.10}.$$

The constant E_0 is the electric field set as the criterion to define the critical current I_c. The typical range for E_0 is 10^{-4} to 10^{-5} V/m (corresponding to more common units of 1 to 0.1 μV/cm). The constant n in Eq. (3.10) defines the electric field dependence on current in the proximity of the I_c transition. Strands and cables with uniform properties are characterised by a large value of n, of the order of 10 and above.

To obtain a general expression for the Joule heat dissipation in the composite component containing a superconductor we distinguish the superconducting cross section A_{sc} from the other (stabilizing) materials, with a total cross section A_{st}. For these last we define an equivalent resistrivety η_{st} in accordance with Eq. (3.6). The total current in the component I_i splits in a part through the superconductor I_{sc} and a part in the stabilizer $I_{st} = I_i - I_{sc}$ such that the longitudinal electric field in both components is identical. The split itself depends on the non linear voltage-current relation for the superconductor, which could be different from Eq. (3.10) as the measurements used to establish it contain the contributions of both superconductor and stabilizer to the longitudinal voltage. In principle a relation of the type of Eq. (3.10) can be obtained from measurements for the superconductor only, correcting for the current sharing in the stabilizer. However it can be shown that in the range of E_0 and n parameters given above the current flowing in the stabilizer is small. Therefore we can safely assume that Eq. (3.10) is valid for the superconductor alone, substituting the total current in the component with the current in the superconductor, i.e.:

$$E_i = E_0 \left(\frac{I_{sc}}{I_c} \right)^n \tag{3.11}.$$

The longitudinal voltage equality in the superconductor and in the stabilizer can be therefore written as follows:

$$\eta_{st} \frac{I_i - I_{sc}}{A_{st}} = E_0 \left(\frac{I_{sc}}{I_c} \right)^n \tag{3.12}.$$

Equation (3.12) can be solved by an iterative technique (see Appendix A) to obtain I_{sc}. The longitudinal electric field is then readily obtained using Eq. (3.11), and the total Joule heat dissipation is given by Eq. (3.7).

Note finally that in accordance to the power law dependence in Eq. (3.11), the electric field is small below the critical current density, rising very quickly to large values above I_c. For this reason this dependence is often modelled as a step function, with a step from zero to infinite electric field located at I_c. Here we prefer to retain the non-linear expression above for generality, still with the possibility to specialize it to the simpler case of a step in the electric field that can be obtained choosing a very large n (ideally infinite).

3.2 Thermal Resistances

In Eq. (3.1) we have introduced the thermal resistance among two thermal components H_{ij} to model thermal coupling within a cable. The corresponding values can be estimated in the case of soldered cables, where the thermal coupling takes place through thermal conduction. Such an estimate is not possible in the case when the thermal coupling takes place through contact surfaces, such as in multi-strand Rutherford or bundled cables. Lacking experimental measurements of thermal resistances, estimates can be obtained assuming that the electrical and thermal contact resistances are correlated through the Wiedeman-Franz-Lorenz law [2]:

$$H_{ij} = \frac{R_{ij}}{L_0 T} \tag{3.13}$$

where R_{ij} is the interstrand resistance per unit length, L_0 is the Lorenz number ($2.45\ 10^{-8}$ [$\Omega W/K^2$]) and T is the average temperature of the two components. In this manner we profit from the fact that the electrical resistance is a key parameter for AC loss considerations, and is therefore often available through measurements or estimates for multi-strand cables. We stress that the above approximation is justified only to evaluate orders of magnitude. The analogy to a conductive material is not necessarily verified, and important effects such as surface contact nature (e.g. sintering) or the presence of stagnant helium permeating a cable are not taken into account.

3.3 Boundary Conditions

Boundary conditions for the thermal problem can be of two types: prescribed temperature or prescribed heat flux. The first case, prescribed temperature, is expressed as:

$$T_i = T_{boundary} \tag{3.14}$$

where $T_{boundary}$ is the temperature at the boundary. In the case of prescribed flux we write:

$$-A_i k_i \frac{\partial T_i}{\partial x} = q_{boundary} \tag{3.15}$$

where $q_{boundary}$ is the heating power at the boundary. Adiabatic conditions are obtained if $q_{boundary}$=0.

4 Hydraulic Components

The flow model is written for a set of parallel, 1-D channels that can exchange mass, momentum and energy among them. The coupling of the channels can happen either through convection heat transfer at the mutual interface, or through direct mass transfer from one flow to the other. In Appendix B we detail how to obtain the set of the three following equations for the volumetric flow $V_h = A_h v_h$, the pressure p_h, and the temperature T_h of the coolant:

$$\rho_h \frac{\partial V_h}{\partial t} + \frac{\rho_h V_h}{A_h}\frac{\partial V_h}{\partial x} + A_h \frac{\partial p_h}{\partial x} - \frac{\rho_h V_h^2}{A_h^2}\frac{\partial A_h}{\partial x} = -A_h F_h - \sum_{\substack{k=1 \\ k\neq h}}^{H} \left(\Gamma_{hk}^v - v_h \Gamma_{hk}^\rho\right) \tag{4.1}$$

$$\begin{aligned} &A_h \frac{\partial p_h}{\partial t} + V_h \frac{\partial p_h}{\partial x} + \rho_h c_h^2 \frac{\partial V_h}{\partial x} = \\ &-\sum_{\substack{k=1 \\ k\neq h}}^{H} \left\{ c_h^2 \Gamma_{hk}^\rho + \varphi_h \left[\Gamma_{hk}^e - v_h \Gamma_{hk}^v - \left(h_h - \frac{v_h^2}{2} \right) \Gamma_{hk}^\rho \right] \right\} + \varphi_h V_h F_h + \varphi_h \dot{q}_h' + \varphi_h \dot{q}_{cf,h}' \end{aligned} \tag{4.2}$$

$$\begin{aligned} &A_h \rho_h C_h \frac{\partial T_h}{\partial t} + \rho_h V_h C_h \frac{\partial T_h}{\partial x} + \rho_h \varphi_h C_h T_h \frac{\partial V_h}{\partial x} = \\ &V_h F_h - \sum_{\substack{k=1 \\ k\neq h}}^{H} \left[\Gamma_{hk}^e - v_h \Gamma_{hk}^v - \left(h_h - \frac{v_h^2}{2} - \varphi_h C_h T_h \right) \Gamma_{hk}^\rho \right] + \dot{q}_h' + \dot{q}_{cf,h}' \end{aligned} \tag{4.3}.$$

where A_h is the cross section of the channel (in principle variable along the length), ρ_h, is the density and v_h is the velocity of the coolant in the channel. The total number of channels is H. The equations above are written using the isentropic sound speed c_h, the specific heat at constant volume C_h, the specific enthalpy h_h and the Gruneisen parameter φ_η. These are tabulated properties for fluids, or can be obtained from the equation from state using known thermodynamic relations [3]. The equations above do not contain any approximations with respect to the conservative form and they are valid for any coolant fluid.

The quantity F_h is the friction force defined using the friction factor f_h and the hydraulic diameter D_h as:

$$F_h = 2\rho_h \frac{f_h}{D_h} v_h |v_h| \tag{4.4}$$

The quantities Γ^{ρ}_{hk}, Γ^{v}_{hk} and Γ^{e}_{hk} are the distributed sources of mass, momentum and stagnation enthalpy per unit length of channel, originating from expulsion (or injection) of helium into (or from) another channel with index k. The convention assumed is that the fluxes are positive if they correspond to a net massflow from channel h to channel k. Finally the source terms $\dot{q}'_h$ and $\dot{q}'_{cf,h}$ represent respectively the heat that enters the channel h per unit length through external sources and convection at the wetted perimeter and the heat flux due to the counterflow mechanism in superfluid conditions.

4.1 External Source Terms

The external source for the flow are represented by a generic heat deposition (retained for generality) and by the heat transfer at the wetted perimeter of the channel, in contact with thermal components through wetted walls. We write the generic source term as:

$$\dot{q}'_h = \dot{q}'_{ext,h} + \sum_{i=1}^{N} p_{ih} h_{ih} \left(T_i - T_h \right) \tag{4.5}$$

where the first term on the r.h.s. is the external heating and the sum is extended on the N thermal components of index i in thermal contact with the channel h, p_{ih} is the wetted perimeter, h_{ih} is the heat transfer coefficient and T_i is the wall temperature.

4.2 Counterflow Heat Exchange in Superfluid Helium

The counterflow heat transport mechanism is peculiar of heat transfer in superfluid helium (or helium II). We can write generically that this term has a form of a non-linear diffusion [4]:

$$\dot{q}'_{cf,h} = \frac{\partial}{\partial x} \left(A_h \widetilde{k}_h \frac{\partial T_h}{\partial x} \right) \tag{4.6}$$

where $\widetilde{k}_h$ is an equivalent thermal conductivity defined using the superfluid thermal conductivity function κ_h as:

$$\widetilde{k}_h = \frac{\kappa_h}{\left(\frac{\partial T_h}{\partial x}\right)^{\frac{2}{3}}} \tag{4.7}.$$

4.3 Transverse Fluxes

To give an explicit expression for the transverse fluxes we indicate with v_{hk} the transverse velocity from channel h to channel k, and we assume that the two channels have a boundary delimited by a perimeter p_{hk} of which the fraction π_{hk} is perforated. We can write:

$$\Gamma^{\rho}_{hk} = \pi_{hk} p_{hk} v_{hk} \overline{\rho} = \dot{m}_{hk} \tag{4.8}$$

$$\Gamma^{v}_{hk} = \pi_{hk} p_{hk} v_{hk} \overline{\rho v} = \dot{m}_{hk} \overline{v} \tag{4.9}$$

$$\Gamma^{e}_{hk} = \pi_{hk} p_{hk} v_{hk} \overline{\rho}\left(\overline{h} + \frac{\overline{v}^2}{2}\right) + p_{hk} h_{hk} \left(T_h - T_k\right) = \dot{m}_{hk}\left(\overline{h} + \frac{\overline{v}^2}{2}\right) + p_{hk} h_{hk} \left(T_h - T_k\right) \tag{4.10}$$

where $\dot{m}_{hk}$ is the massflow from channel h to channel k per unit channel length. We assume that the transverse flow between the channels can be modelled as a discharge between two volumes at different pressure. The transverse flow velocity v_{hk} is then given by:

$$v_{hk} = \alpha_{hk}\left(p_h - p_k\right) \tag{4.11}$$

where the coefficient α_{hk} is given by:

$$\alpha_{hk} = \sqrt{\frac{2}{\overline{\rho}\left|p_h - p_k\right|}} \tag{4.12}$$

The overbar quantities in the equations above are intended as upwinded, i.e. taken from the upstream conditions of the transverse flow, or:

$$\overline{\rho} = \begin{cases} \rho_h & \text{for } p_h \geq p_k \\ \rho_k & \text{for } p_h < p_k \end{cases} \tag{4.13}$$

$$\overline{v} = \begin{cases} v_h & \text{for } p_h \geq p_k \\ v_k & \text{for } p_h < p_k \end{cases} \tag{4.14}$$

$$\bar{h} = \begin{cases} h_h & \text{for } p_h \geq p_k \\ h_k & \text{for } p_h < p_k \end{cases} \tag{4.15}$$

In Eq. (4.10) the two terms take into account the fact that energy transfer between the two channels can happen either through mass convection (first term on the r.h.s.), or through heat transfer at the boundary (second term on the r.h.s.). The heat transfer happens on the interface perimeter p_{hk} with an equivalent heat transfer coefficient h_{hk}.

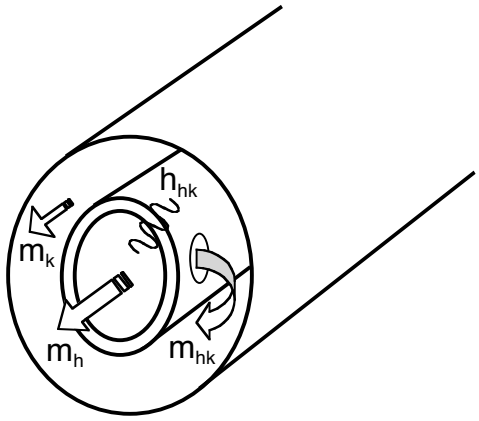

Figure 4. Schematic representation of the coupling between two parallel cooling channels h and k. The channels exchange mass through a set of perforations, and can exchange heat through the wall. The wall can be fictitious, and the shape of the channel and perforations is irrelevant.

4.4 Heat Transfer Models

The heat transfer coefficients h_{ih} between the coolant in channel h and the solid wall i, or h_{hk} between coolant flows h and k are computed using empirical correlations. At present this is the most general approach as it relies on experimental data. The correlation models for the heat transfer coefficient have typical data fitting accuracy in the range of some 10 %, and predictive capability within a factor 2. See [5] for a database of heat transfer correlations that apply to helium.

4.5 Friction Factor Models

Similarly to the heat transfer coefficient, the friction factor of the flow is computed based on empirical correlations. The correlation models for the friction factor coefficient have data fitting accuracy within a factor 2. See [6] for a database of friction factor correlations that apply to helium.

4.6 Boundary Conditions

The imposition of boundary conditions to the fluid flow is a delicate matter, that should take into account the characteristics at the boundary [7]. We have found that in the non-conservative form described above it is possible to impose accurate boundary conditions in a simpler manner if we limit our choice to a a closed pipe condition, or alternatively to in- and outflow into a volume at given pressure and temperature [8]. The first case (closed pipe) is imposed setting:

$$V_h = 0 \tag{4.16}.$$

In the second case, volume in- and out-flow, we match the number of conditions imposed to the number of characteristics entering or exiting the boundary surface. Separate treatment is necessary in the case of a normal or superfluid flow, as in the case of superfluid the equations have a parabolic term. We have the following possibilities:

4.6.1 Subsonic inflow ($v_h < c_h$).

In this case we have 2 entering characteristics, 1 exiting characteristic. Two variables are specified

$$p_h = p_{boundary} \tag{4.17}$$

$$T_h = T_{boundary} \tag{4.18}$$

where $p_{boundary}$ and $T_{boundary}$ are the values of pressure and temperature at the boundary.

4.6.2 Supersonic inflow ($v_h > c_h$).

For supersonic inflow we have 3 entering characteristics and no exiting characteristic. Three variables must be specified:

$$p_h = p_{boundary} \tag{4.19}$$

$$T_h = T_{boundary} \tag{4.20}$$

$$V_h = A_{boundary} c_{boundary} \tag{4.21}$$

where $c_{boundary}$ is the sound speed at the boundary.

4.6.3 Subsonic outflow ($v_h < c_h$).

In this case we have 1 entering characteristic, 2 exiting characteristics. For a flow of normal fluid only one variable can be specified:

$$p_h = p_{boundary} \tag{4.22}.$$

In the case of superfluid it is in addition necessary to specify the boundary temperature:

$$T_h = T_{boundary} \tag{4.23}.$$

4.6.4 Supersonic outflow ($v_h > c_h$).

For supersonic outflow there is no entering characteristic and 3 exiting characteristics. In this case no boundary condition can be specified in the case of a normal flow. For convenience this rare case is dealt in the same manner also in case of superfluid.

5 Electric Components

The electric model describes a cable subdivided in E parallel, electrically conductive components characterised by a non-linear longitudinal resistance, mutual and self inductance. Within the frame of the model the generic component can be a single strands, a cable subunit, a segregated stabilizer, or any electrically conducting structural component. Each component has a constant current density in its cross section, and current transfer happens along the length of the cable in a continuous manner through distributed electrical conductances.

The equations governing the evolution of the currents in the components are derived in Appendix C. They are written in the following matrix form:

$$\mathbf{l}\frac{\partial \mathbf{I}}{\partial t} + \mathbf{r}\mathbf{I} - \frac{\partial}{\partial x}\left(\mathbf{c}^{-1}\frac{\partial \mathbf{I}}{\partial x}\right) = \Delta \mathbf{v}^{ext} \tag{5.1}.$$

where the unknowns are the currents I_e in the components, packed in the array **I**. The matrices and vectors depend on the cable geometry (e.g. inductance), its properties (e.g. transverse conductivity) and on the operating conditions (e.g. parallel resistance and flux changes).

5.1 Coupling with Thermal Components

The electric model is coupled to the heat conduction model described earlier. Unlikely the cases examined so far, the electric-thermal coupling is largely implicit. The main coupling between the two domains is based on the fact that the longitudinal resistance appearing in the matrix **r** of the electric model depends on the temperature computed in the heat conduction model, while the current I_i and thus the Joule heat generation in the thermal component depends on the current distribution computed in the electric model. In addition the current transfer among the components takes place in the transverse electrical conductances. This is associated with a Joule heating $\dot{q}'_{transverse,e}$ in each electric component as described in Appendix E.

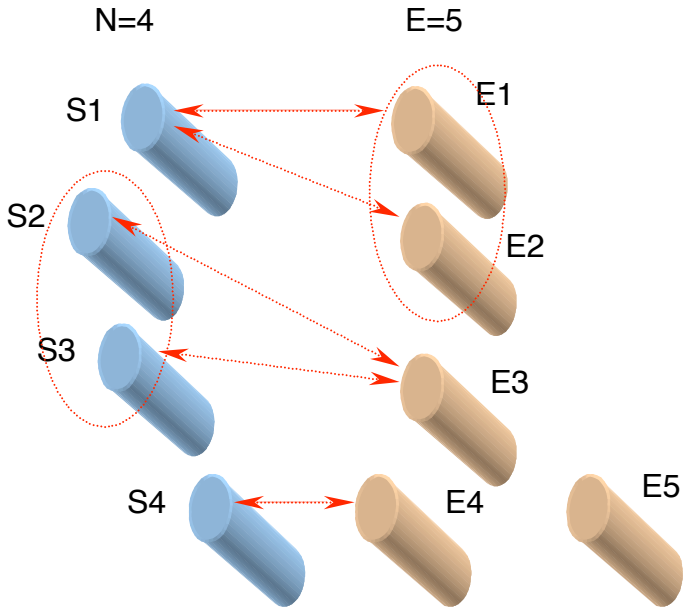

Figure 5. Schematic view of possible coupling of N thermal components (on the left) and E electric components (on the right). The thermal components can be coupled to one, several or no electric components, and similarly electric components can be coupled to one, several or no thermal component. Ordering is inessential. The electric components E1 and E2 are *grouped*, and it is not possible to couple them to other thermal components than S1. Similarly, the thermal components S2 and S3 are grouped, and cannot be coupled to any other electric component in addition to E3.

The coupling in the frame of our model is obtained matching a set of electric components to corresponding thermal components. For generality we assume that the matching is not necessarily one-to-one, i.e. a single electric component can model the current flow in several parallel thermal components, or conversely one thermal component can model the temperature evolution in several parallel electric components. The components of one domain (thermal or electric) that are associated to a single component in the other domain (electric or thermal) are said to be *grouped*. To avoid inconsistencies in the total power dissipation between the thermal and electric models we prevent the possibility of coupling the same grouped components to more than one component in the other domain. The most general case of a set of N thermal

components associated with E electric components is shown schematically in Fig. 5. As we prevent multiple coupling of groups, we can only have the following three cases:

- coupling of a single thermal and electric component (e.g. S4 coupled to E4 in Fig. 5)
- a group of electric components is coupled to a thermal component component (e.g. S4 coupled to E1 and E2 in Fig. 5)
- a group of solid components is coupled to an electric component (e.g. S2 and S3 coupled to E3 in Fig. 5)

In the case of coupling of a single thermal and electric components, the current is transferred directly from one to the other:

$$I_i = I_e \tag{5.2}$$

as well as the transverse Joule power per unit length:

$$\dot{q}'_{transverse,i} = \dot{q}'_{transverse,e} \tag{5.3}.$$

The resistance per unit length of the electric component is calculated as:

$$r_e = \frac{\eta_i}{A_i} \tag{5.4}.$$

If a group of E_i of electric components is coupled to the thermal component i we compute the current in the thermal component as the sum of all the currents in the coupled electric components:

$$I_i = \sum_{e \in Ei} I_e \tag{5.5}$$

where the index e scans the group E_i. The same sum is used for the transverse Joule heat per unit length:

$$\dot{q}'_{transverse,i} = \sum_{e \in Ei} \dot{q}'_{transverse,e} \tag{5.6}.$$

The resistance of the electric components is obtained assuming a regular subdivision of the cross section:

$$r_e = \frac{\eta_i}{A_i} E_i \tag{5.7}$$

which guarantees that the parallel of the longitudinal resistances is identical in the thermal and electric model, but does not necessarily guarantee that the Joule heat associated with the longitudinal electric field is the same in the two models.

In the third case, of a group of thermal components N_e coupled to a single electric component e, we distribute the current assuming that the current sharing among thermal components is purely resistive. To achieve this we compute first the parallel resistance per unit length of the group of thermal components, and transfer it to the electric component:

$$\frac{1}{r_e} = \sum_{i \in Ne} \frac{A_i}{\eta_i} \tag{5.8}.$$

The current I_e is then obtained:

$$I_i = \frac{A_i}{\eta_i} I_e r_{Ne} \tag{5.9}.$$

In case of a parallel of superconducting thermal components the resistance of each component is zero, and the total resistance is also zero. The weighting in Eq. (5.9) becomes singular. In this case we choose to assign a small but finite resistance ε to each superconducting component, thus achieving a equal distribution of the total current among all superconducting components without affecting the evolution of the current. Finally, the transverse Joule heat is distributed equally among all thermal components:

$$\dot{q}'_{transverse,i} = \frac{\dot{q}'_{transverse,e}}{N_e} \tag{5.10}.$$

Note that this assumption conserves the total transverse power generated, but it is not necessarily consistent with the split of current among the thermal components.

5.2 Boundary Conditions

We ideally consider that all electric components are singularly powered at the cable ends. The boundary conditions that can be applied to the electric model are of two types: imposed current or voltage difference.

The first condition corresponds to having a current source for each electric component, resulting in a boundary condition:

$$I_e = I_{boundary} \tag{5.11}$$

where $I_{boundary}$ is the current at the boundary. In any case the total current must be conserved at the boundaries, and this implies for consistence that the above boundary condition can only be imposed on E-1 of the E electric components (see Appendix D). An open circuit condition can be obtained from this boundary type setting $I_{boundary}$=0.

In the second case a voltage source is applied among all couples of electric components, i.e. the following condition is used at the boundary:

$$\Delta v_e^{ext} = \Delta v_e^{ext} + \Delta v_{boundary} \tag{5.12}$$

where the applied voltage term $\Delta v_{boundary}$ modifies all boundary entries in the applied voltage vector $\Delta \mathbf{v}^{\text{ext}}$. If all components are in short, the voltage differences are by definition zero and the boundary condition Eq. (5.12) is equivalent to (see Appendix D):

$$\frac{\partial I_e}{\partial x} = 0 \tag{5.13}.$$

6 Matrix Form

The equations presented so far are numerous and cumbersome to treat singularly. It is much more convenient to write in the following compact form for a system of Partial Differential Equations (PDE's) amenable of unified treatment:

$$\mathbf{m}\frac{\partial \mathbf{u}}{\partial t} + \mathbf{a}\frac{\partial \mathbf{u}}{\partial x} - \frac{\partial}{\partial x}\left(\mathbf{g}\frac{\partial \mathbf{u}}{\partial x}\right) + \mathbf{s}\mathbf{u} = \mathbf{q} \tag{6.1}$$

where the vector of unknowns $\mathbf{u}(x,t)$ is defined assembling the unknowns of each PDE as derived for heat conduction in the N solids, conservation balances in the H cooling channels and current distribution among E conducting materials, i.e.:

$$\mathbf{u} = \begin{bmatrix} \frac{T_i}{V_h} \\ p_h \\ \frac{T_h}{I_e} \end{bmatrix} \tag{6.2}.$$

The vector **u** has therefore size *N+H+E*. The matrices appearing in Eq. (6.1) have a general block structure that we can define using the matrix **m** as an example:

$$\mathbf{m} = \begin{bmatrix} \mathbf{m}_i & \mathbf{m}_{ih} & 0 \\ \mathbf{m}_{hi} & \mathbf{m}_h & 0 \\ 0 & 0 & \mathbf{m}_e \end{bmatrix} \tag{6.3}$$

Each block is intended as a matrix itself, blocks on the diagonal are the contributions from the three different coupled problems (thermal, hydraulic and electric) and blocks outside the diagonal represent coupling between the problems. Note that with the structure chosen above we have decoupled the electric problem, as indicated by the zero coupling terms on the last row and column in the matrix. Each matrix block can be built by identification of Eqs. (6.1) with the corresponding terms in the models discussed previously. Explicitly, we obtain (the matrix entry is written for a single component):

$$\mathbf{m}_i = \left[\rho_i A_i C_i\right] \tag{6.4}$$

$$\mathbf{m}_{ih} = \left[0\right] \tag{6.5}$$

$$\mathbf{m}_{hi} = \left[0\right] \tag{6.6}$$

$$\mathbf{m}_h = \begin{bmatrix} \rho_h & 0 & 0 \\ 0 & A_h & 0 \\ 0 & 0 & A_h \rho_h C_h \end{bmatrix} \tag{6.7}$$

$$\mathbf{m}_e = \mathbf{l} \tag{6.8}$$

$$\mathbf{a}_i = \left[0\right] \tag{6.9}$$

$$\mathbf{a}_{ih} = \left[0\right] \tag{6.10}$$

$$\mathbf{a}_{hi} = \left[0\right] \tag{6.11}$$

$$\mathbf{a}_h = \begin{bmatrix} \rho_h v_h & A_h & 0 \\ \rho_h c_h^2 & A_h v_h & 0 \\ \rho_h \varphi_h C_h T_h & 0 & A_h \rho_h v_h C_h \end{bmatrix} \tag{6.12}$$

$$\mathbf{a}_e = \left[0\right] \tag{6.13}$$

$$\mathbf{g}_i = \left[A_i k_i \right] \tag{6.14}$$

$$\mathbf{g}_{ih} = \left[0 \right] \tag{6.15}$$

$$\mathbf{g}_{hi} = \left[0 \right] \tag{6.16}$$

$$\mathbf{g}_h = \begin{bmatrix} 0 & 0 & 0 \\ 0 & 0 & A_h \varphi_h \widetilde{k}_h \\ 0 & 0 & A_h \widetilde{k}_h \end{bmatrix} \tag{6.17}$$

$$\mathbf{g}_e = \mathbf{c}^{-1} \tag{6.18}$$

$$\mathbf{s}_i = \begin{bmatrix} p_{ij} h_{ij} & -p_{ij} h_{ij} \\ -p_{ij} h_{ij} & p_{ij} h_{ij} \end{bmatrix} \tag{6.19}$$

$$\mathbf{s}_{ih} = \begin{bmatrix} p_{ih} h_{ih} & 0 & 0 & -p_{ih} h_{ih} \end{bmatrix} \tag{6.20}$$

$$\mathbf{s}_{hi} = \begin{bmatrix} 0 & 0 & 0 & 0 \\ -\varphi_h p_{ih} h_{ih} & 0 & 0 & \varphi_h p_{ih} h_{ih} \\ -p_{ih} h_{ih} & 0 & 0 & p_{ih} h_{ih} \end{bmatrix} \tag{6.21}$$

$$\mathbf{s}_h = \mathbf{s}_h^f + \mathbf{s}_h^{\Delta p} + \mathbf{s}_h^{\Delta T} \tag{6.22}$$

$$\mathbf{s}_h^f = \begin{bmatrix} 2\frac{\rho_h f_h}{D_h} |v_h| - \frac{\rho_h v_h}{A_h} \frac{\partial A_h}{\partial x} & 0 & 0 \\ -2\varphi_h \frac{\rho_h f_h}{D_h} |v_h| v_h & 0 & 0 \\ -2\frac{\rho_h f_h}{D_h} |v_h| v_h & 0 & 0 \end{bmatrix} \tag{6.23}$$

$$\mathbf{s}_h^{\Delta p} = \begin{bmatrix} 0 & \chi_{hk}(\overline{v}-v_h) & 0 & 0 & -\chi_{hk}(\overline{v}-v_h) & 0 \\ 0 & \varphi_h\chi_{hk}\left(\overline{h}-h_h+\frac{(\overline{v}-v_h)^2}{2}+\frac{c_h^2}{\varphi_h}\right) & 0 & 0 & -\varphi_h\chi_{hk}\left(\overline{h}-h_h+\frac{(\overline{v}-v_h)^2}{2}+\frac{c_h^2}{\varphi_h}\right) & 0 \\ 0 & \chi_{hk}\left(\overline{h}-h_h+\frac{(\overline{v}-v_h)^2}{2}+\varphi_h C_h T_h\right) & 0 & 0 & -\chi_{hk}\left(\overline{h}-h_h+\frac{(\overline{v}-v_h)^2}{2}+\varphi_h C_h T_h\right) & 0 \\ 0 & -\chi_{hk}(\overline{v}-v_k) & 0 & 0 & \chi_{hk}(\overline{v}-v_k) & 0 \\ 0 & -\varphi_k\chi_{hk}\left(\overline{h}-h_k+\frac{(\overline{v}-v_k)^2}{2}+\frac{c_k^2}{\varphi_k}\right) & 0 & 0 & \varphi_k\chi_{hk}\left(\overline{h}-h_k+\frac{(\overline{v}-v_k)^2}{2}+\frac{c_k^2}{\varphi_k}\right) & 0 \\ 0 & -\chi_{hk}\left(\overline{h}-h_k+\frac{(\overline{v}-v_k)^2}{2}+\varphi_k C_k T_k\right) & 0 & 0 & \chi_{hk}\left(\overline{h}-h_k+\frac{(\overline{v}-v_k)^2}{2}+\varphi_k C_k T_k\right) & 0 \end{bmatrix} \tag{6.24}$$

where we have used for convenience:

$$\chi_{hk} = \alpha_{hk}\pi_{hk}p_{hk}\overline{\rho} \tag{6.25}$$

$$\mathbf{s}_h^{\Delta T} = \begin{bmatrix} 0 & 0 & 0 & 0 & 0 & 0 \\ 0 & 0 & \varphi_h p_{hk} h_{hk} & 0 & 0 & -\varphi_h p_{hk} h_{hk} \\ 0 & 0 & p_{hk} h_{hk} & 0 & 0 & -p_{hk} h_{hk} \\ 0 & 0 & 0 & 0 & 0 & 0 \\ 0 & 0 & -\varphi_k p_{hk} h_{hk} & 0 & 0 & \varphi_k p_{hk} h_{hk} \\ 0 & 0 & -p_{hk} h_{hk} & 0 & 0 & p_{hk} h_{hk} \end{bmatrix} \tag{6.26}$$

$$\mathbf{s}_e = \mathbf{r} \tag{6.27}$$

$$\mathbf{q}_i = \left[q_i'\right] \tag{6.28}$$

$$\mathbf{q}_h = \begin{bmatrix} 0 \\ \varphi_h q_h' \\ q_h' \end{bmatrix} \tag{6.29}$$

$$\mathbf{q}_e = \Delta\mathbf{v}^{ext} \tag{6.30}$$

7 Solution Strategy

For the solution of the system of PDE's of Eq. (6.1) we have chosen to use independent space and time discretizations. The discretization in space is done using variable order lagrangian finite elements, while in time we discretize using a multi-step finite difference algorithm.

7.1 Space Discretization

For the discretization in space we subdivide the 1-D domain in an arbitrary number of finite elements[9]. Each node of the mesh has a number of degrees of freedom (DOF's) equal to the total number of variables in the system Eq. (6.1).

Meshing in space is automatic and adaptive, to resolve fine details with space scale in the range of 1 mm in a mesh that can be as long as 1 km. Adaptivity is based on:

- user specified refinements;
- tracking of discontinuities and travelling fronts;
- minimization of the interpolation error.

The algorithm for meshing is an extension of the one described in [8]. The new mesh is generated at each time step based on a *mesh density* profile established on the mesh used for the solution at the previous time step. We have chosen to use a pure '*h*' refinement (element size), rather than a combination with '*p*' refinement (element order). Therefore the mesh consists of only one type of element. Furthermore, within each element the nodes spacing is uniform in x in order to avoid singularities in the transformation between the parent plane and the physical plane. The definition of the mesh density profile and the procedure for mesh generation are described in Appendix F.

On the 1-D mesh we approximate the system variables using shape functions **N**:

$$\mathbf{u} \approx \mathbf{N}\mathbf{U} \tag{7.1}$$

where **U** is the vector formed by the values of the variables at the nodes of the finite element mesh. See Appendix G for details on the shape functions of the finite elements chosen. The space discretization is obtained by weighted integration, using weight functions equal to the shape functions (Bubnov-Galerkin method). As a result the system of PDE's (6.1) gives origin to the following system of ODE's:

$$\mathbf{M}\frac{\partial \mathbf{U}}{\partial t} + \left[\mathbf{A} + \mathbf{G} + \mathbf{S}\right]\mathbf{U} = \mathbf{Q} \tag{7.2}$$

where the matrices appearing above are obtained by assembly of the element contributions of the following integrals:

$$\mathbf{M} = \int \mathbf{N}^T \mathbf{m} \mathbf{N}\, dx \tag{7.3}$$

$$\mathbf{A} = \int \mathbf{N}^T \mathbf{a} \frac{\partial \mathbf{N}}{\partial x} dx \tag{7.4}$$

$$\mathbf{G} = \int \frac{\partial \mathbf{N}^T}{\partial x} \mathbf{g} \frac{\partial \mathbf{N}}{\partial x} \, dx \tag{7.5}$$

$$\mathbf{S} = \int \mathbf{N}^T \mathbf{s} \mathbf{N} \, dx \tag{7.6}$$

$$\mathbf{Q} = \int \mathbf{N}^T \mathbf{q} \, dx \tag{7.7}.$$

The integrals are performed using Gauss integration, which is necessary to deal with non-linearities in the matrices of coefficients as well as variable order interpolation in the mesh. The detailed procedure for the Gauss integration of the matrices above is given in Appendix H.

7.2 Time Discretization

The system of ODE's Eq. (7.2) is solved with a multi-step algorithm of the Beam and Warming family [10]. We write the system in the following simpler form:

$$\mathbf{M} \frac{\partial \mathbf{U}}{\partial t} + \mathbf{H}\mathbf{U} = \mathbf{Q} \tag{7.8}$$

where we have introduced the matrix **H** equal to the sum of the matrices **A**, **G** and **S**. The time discretization is performed as follows:

$$(1+\xi)\mathbf{M} \frac{\mathbf{U}^{n+1} - \mathbf{U}^n}{\Delta t^n} - \xi \mathbf{M} \frac{\mathbf{U}^n - \mathbf{U}^{n-1}}{\Delta t^{n-1}} + \theta \mathbf{H}\left(\mathbf{U}^{n+1} - \mathbf{U}^n\right) + \mathbf{H}\mathbf{U}^n + \phi \mathbf{H}\left(\mathbf{U}^n - \mathbf{U}^{n-1}\right) = \mathbf{Q} \tag{7.9}$$

where superscripts *n-1*, *n* and *n+1* indicate variables at the corresponding time stations during integration, Δt^{n-1} and Δt^n are the time steps from time stations *n-1* to *n* and from *n* to *n+1* respectively. To linearise the solution of Eq. (7.9) all matrices and loads are evaluated from the known value $\mathbf{U}^n$ and at a time t^*:

$$t^* = t^n + \theta \Delta t^n - \phi \Delta t^{n-1} \tag{7.10}.$$

We now introduce the increments of the variable **U** between the time stations:

$$\Delta \mathbf{U}^{n-1} = \mathbf{U}^n - \mathbf{U}^{n-1} \tag{7.11}$$

and

$$\Delta \mathbf{U}^n = \mathbf{U}^{n+1} - \mathbf{U}^n \tag{7.12}$$

and we rewrite the system of algebraic equations Eq. (7.9) as follows:

$$\left[(1+\xi)\mathbf{M}+\theta\Delta t^n\mathbf{H}\right]\Delta\mathbf{U}^n=\left[\xi\frac{\Delta t^n}{\Delta t^{n-1}}\mathbf{M}-\phi\Delta t^n\mathbf{H}\right]\Delta\mathbf{U}^{n-1}-\Delta t^n\mathbf{H}\mathbf{U}^n+\Delta t^n\mathbf{Q} \qquad (7.13).$$

The parameters ξ, θ and ϕ must be chosen so that the method is consistent and achieves the desired accuracy. Depending on the choice of the set of parameters, several known numerical schemes can be obtained. A list of possible choices is given in Tab. 1, together with the numerical accuracy order achieved.

Table 1. Choice of numerical parameters for the time integration scheme and corresponding time accuracy.

ξ	θ	ϕ	order of accuracy	method
0	1	0	1	Euler-backward
0	1/2	0	2	Crank-Nicolson
1/2	1	0	2	Backward differences
-1/6	1/3	0	3	3rd order implicit
0	5/12	1/12	3	Adams-Moulton
-1/2	1/6	-1/6	4	Milne

7.3 Artificial Viscosity

The system Eqs. (6.1) has a mixed parabolic-hyperbolic nature, and is known to generate oscillatory solutions whenever the hyperbolic character dominates. This can happen in practice in two instances. At low Mach numbers oscillations can appear in the vicinity of temperature and density discontinuities that are propagated at the speed of the flowing coolant. In this case the oscillations tend to grow only in the presence of strong non-linearities such as a quench front. These oscillations can be effectively reduced using denser meshes and mesh adaptivity.

The second situation in which the flow equations are dominatd by the hyperbolic terms is in the presence of pressure and shock waves at high Mach numbers. In this case the oscillations appear at the propagating pressure front, and tend to grow in time due to the non-linear interaction among the mass, momentum and energy balance in the coolant. These non-physical oscillations can lead to wrong wave or shock propagation speed, and can cause divergence of the solution. Experience has shown that in this case the addition of a diffusive term of the form due to Lapidus [11]:

$$\cdots-\frac{\partial}{\partial x}\left(C_{Lapidus}\Delta x^2\left|\frac{\partial v_h}{\partial x}\right|\frac{\partial V_h}{\partial x}\right) \qquad (7.14)$$

to the momentum balance gives monotonic results with acceptable smoothing and maintaining second order accuracy in space. In Eq. (7.14) the constant $C_{Lapidus}$ is in the range of unity, and Δx is the element size. The gradient is evaluated only for the variables that have hyperbolic character, i.e. the flow variables. As the term above is only added to the momentum balance, the group $C_{Lapidus}\Delta x^2\left|\frac{\partial v_h}{\partial x}\right|$ is often referred to as *artificial viscosity*. The term in Eq. (7.14) results in the addition of the following modification to the matrix $\mathbf{g}_h$:

$$\mathbf{g}_{AV} = \begin{bmatrix} \rho_h C_{Lapidus}\Delta x^2\left|\frac{\partial v_h}{\partial x}\right| & 0 & 0 \\ \varphi_h v_h \rho_h C_{Lapidus}\Delta x^2\left|\frac{\partial v_h}{\partial x}\right| & 0 & 0 \\ v_h \rho_h C_{Lapidus}\Delta x^2\left|\frac{\partial v_h}{\partial x}\right| & 0 & 0 \end{bmatrix} \tag{7.15}$$

7.4 System Solution

The system of equations Eq. (7.13) is in the form of a standard algebraic system for the increment of the unknowns $\Delta\mathbf{U}^n$. The matrix products and vectors on the r.h.s. can be obtained during assembly at the element level. Therefore they do not require the complete assembly of the matrices **M** and **H**. The system matrix on the l.h.s. on the other hand needs to be built for the system solution. However, owing to the sparse structure of the finite element mesh and interpolation functions, this matrix is not full. This feature is exploited storing the system matrix as a non-symmetrical banded matrix. Matrix scaling and double accuracy are necessary to achieve a stable system solution.

8 References

[1] L. Bottura, *Modelling Stability in Superconducting Cables*, Physica C, **310** (1-4), 316-326, 1998.

[2] M.N. Wilson, R. Wolf, *Calculation of Minimum Quench Energies in Rutherford Cables*, IEEE Trans. Appl. Sup., **7** (2), 950-953, 1997 .

[3] V.D. Arp, *Stability and Thermal Quenches in Force-cooled Superconducting Cables*, Proc. of 1980 Superconducting MHD Magnet Design Conference, MIT, 142-157, 1980.

[4] L. Bottura, C. Rosso, *Finite Element Simulation of Steady State and Forced Convection in Superfluid Helium*, Int. J. Num. Methods Fluids, **30**, 1091-1108, 1999.

[5] L. Bottura, *Heat Transfer Correlations*, CryoSoft Internal Note CRYO/98/010, 1999.

[6] L. Bottura, *Friction Factor Correlations*, CryoSoft Internal Note CRYO/98/009, 1999.

[7] C. Hirsch, *Numerical Computation of Internal and External Flows*, J. Wiley & Sons, 1988.

[8] L. Bottura, *A Computational Model for the Simulation of Quench in the ITER Magnets*, J. Comp. Phys., **125**, 26-41, 1996.

[9] O.C. Zienkiewicz, *The Finite Element Method*, 4th edition, McGraw-Hill, 1991.

[10] R.M. Beam, R.F. Warming, *Alternating Direction Implicit Methods for Parabolic Equations with a Mixed Derivative*, SIAM J. Sci. Stat. Comp., **1**, 131-159, 1980.

[11] A. Lapidus *A Detached Shock Calculation by Second Order Finite Differences*, J. Comp. Phys., **2**, 154-177, 1967.

9 Current Sharing Between Superconductor and Stabilizer

We consider in detail the case of a solid component consisting of a superconducting material with cross section A_{sc} in parallel with a stabilizing shunt with cross section A_{st}. The component carryes a total current I. We model the non-linear relation between the longitudinal electric field in the superconducting material E_{sc} and the current density J_{sc} with the following power law:

$$E_{sc} = E_0 \left(\frac{J_{sc}}{J_c} \right)^n \tag{A.1}$$

where the constant E_0 is the electric field cryterion that defines the critical current density J_c, and the constant n is empirical. For large values of the expoonent n we see that the longitudinal electric field in the superconductor is small below the critical current, and increases rapidly above. In correspondance to the change of electric field, the total current flowing in the component I splits in a current I_{sc} flowing in the superconductor and a current I_{st} flowing in the stabilizer. Indicating the stabilizer resistivity with η_{st} we have that the longitudinal field in the stabilizer is given by:

$$E_{st} = \eta_{st} \frac{I_{st}}{A_{st}} \tag{A.2}.$$

Because superconductor and stabilizer are equipotential, the longitudinal electric field along both must be the same and therefore we can write that:

$$\eta_{st} \frac{I_{st}}{A_{st}} = E_0 \left(\frac{I_{sc}}{I_c} \right)^n \tag{A.3}$$

where we have used for convenience the critical current $I_c = A_{sc} J_{sc}$. We now impose that the total current in the component is conserved, so that we can finally derive the following implicit equation for the current in the superconductor:

$$\eta_{st} \frac{I - I_{sc}}{A_{st}} = E_0 \left(\frac{I_{sc}}{I_c} \right)^n \tag{A.4}.$$

To solve Eq. (A.4) we firstly introduce the following normalization:

$$x = \frac{I_{sc}}{I_c} \tag{A.5},$$

$$i = \frac{I}{I_c} \tag{A.6}.$$

Using the definitions above, Eq. (A.4) is finally put in the following form:

$$x^n + a(x - i) = 0 \tag{A.7}$$

where we have defined the constant:

$$a = \frac{\eta_{st} I_c}{A_{st} E_0} \tag{A.8}.$$

Equation (A.7) is of order n, and has therefore in principle n complex roots. In practice we are looking for the single root x in the closed interval $[0 \ldots i]$. The root can be found by the following Newton iteration (subscript i indicates iterated values):

$$x_{i+1} = x_i - \frac{R(x_i)}{J(x_i)} \tag{A.9}.$$

The residual $R(x)$ and Jacobian $J(x)$ of the iteration are defined as follows:

$$R(x) = x^n + a(x - i) \tag{A.10}$$

$$J(x) = nx^{n-1} + ax \tag{A.11}$$

The starting point of the iteration x_0 is very critical to ensure fast convergence, especially for large values of the exponent n. In practice we found that fast convergence can be obtained starting with the following approximation of the root sought:

$$x_0 = \min\left\{1, \sqrt[n]{ai}\right\} \tag{A.12}.$$

Once Eq. (A.7) is solved, the current in the superconductor and in the stabilizer can be obtained from Eq. (A.5) and from the condition on the conservation of the total current. The longitudinal electric field E is then calculated either using Eq. (A.1) or Eq. (A.2). Both equations should lead to the same value, and therefore a comparison of the two results gives a good check on the quality of the iterative solution.

The heat dissipated in the superconductor and in the stabilizer are finally given by

$$q'_{sc} = EI_{sc} \tag{A.13}$$

$$q'_{st} = EI_{st} \tag{A.14}$$

and the total heat dissipated is the sum of the two, or:

$$q' = EI \tag{A.15}.$$

As a complement to the above discussion, it is useful to give the limiting case of the above procedure for a very large (ideally infinite) value of the exponent n. In this case the longitudinal field in the superconductor is zero till the critical current, and is undetermined above it. Correspondingly Eq. (A.7) degenerates, but still has a usable solution:

$$x = \begin{cases} i & for i \le 1 \\ 1 & for i > 1 \end{cases} \tag{A.16}$$

from which again we can compute the longitudinal field and the Joule heating. Note finally that in the case of a linear dependence of the critical current on temperature and constant stabilizer resistivity the limiting case of infinite n results in the approximation commonly made of linear Joule heating dependence between current sharing and critical temperature [Wilson].

10 Non-Conservative Flow Equations

We start from the conservative form of the mass, momentum and energy conservation in a 1-D channel identified by the index *h*:

$$\frac{\partial \rho_h A_h}{\partial t} + \frac{\partial \rho_h A_h v_h}{\partial x} = -\sum_{k=1}^{H} (1-\delta_{hk}) \Gamma_{hk}^{\rho} \tag{B.1}$$

$$\frac{\partial \rho_h A_h v_h}{\partial t} + \frac{\partial \rho_h A_h v_h^2}{\partial x} + A_h \frac{\partial p_h}{\partial x} = -A_h F_h - \sum_{k=1}^{H} (1-\delta_{hk}) \Gamma_{hk}^{v} \tag{B.2}$$

$$\frac{\partial \rho_h A_h e_h}{\partial t} + \frac{\partial \rho_h A_h e_h v_h}{\partial x} + \frac{\partial p_h A_h v_h}{\partial x} = -\sum_{k=1}^{H} (1-\delta_{hk}) \Gamma_{hk}^{e} + \dot{q}_h' + \dot{q}_{cf,h}' \tag{B.3}.$$

For convenience in the following treatment we introduce the volumetric flux:

$$V_h = A_h v_h \tag{B.4}$$

The three conservation balances (B.1), (B.2) and (B.3) can be written:

$$A_h \frac{\partial \rho_h}{\partial t} + \frac{\partial \rho_h V_h}{\partial x} = -\sum_{k=1}^{H} (1-\delta_{hk}) \Gamma_{hk}^{\rho} \tag{B.5}$$

$$\frac{\partial \rho_h V_h}{\partial t} + \frac{\partial \rho_h V_h v_h}{\partial x} + A_h \frac{\partial p_h}{\partial x} = -A_h F_h - \sum_{k=1}^{H} (1-\delta_{hk}) \Gamma_{hk}^{v} \tag{B.6}$$

$$\frac{\partial \rho_h A_h e_h}{\partial t} + \frac{\partial \rho_h V_h e_h}{\partial x} + \frac{\partial p_h V_h}{\partial x} = -\sum_{k=1}^{H} (1-\delta_{hk}) \Gamma_{hk}^{e} + \dot{q}_h' + \dot{q}_{cf,h}' \tag{B.7}$$

To derive a convenient non-conservative form we make use of the following thermodynamic relations between specific internal energy *i*, pressure *p*, density ρ and temperature *T*:

$$di = \left(\frac{p}{\rho} - \varphi C_v T \right) \frac{d\rho}{\rho} + C dT \tag{B.8}$$

$$\left(c^2 - \frac{p\varphi}{\rho} \right) d\rho = dp - \varphi \rho di \tag{B.9}.$$

The relations involve the isentropic sound speed *c*, the specific heat at constant volume *C* and the Gruneisen parameter φ. In addition we remember that the relation between total and internal specific energy is:

$$e = i + \frac{v^2}{2} \tag{B.10}$$

while the specific enthalpy h is related to the internal specific energy by:

$$h = i + \frac{p}{\rho} \tag{B.11}$$

We start now with the momentum balance, Eq. (B.6), subtracting the continuity equation, Eq. (B.5), multiplied by the velocity, and we obtain the momentum balance in non-conservative form:

$$\rho_h \frac{\partial V_h}{\partial t} + \frac{\rho_h V_h}{A_h}\frac{\partial V_h}{\partial x} + A_h \frac{\partial p_h}{\partial x} - \frac{\rho_h V_h^2}{A_h^2}\frac{\partial A_h}{\partial x} = -A_h F_h - \sum_{k=1}^{H}\left(1-\delta_{hk}\right)\left(\Gamma_{hk}^{v} - v_h \Gamma_{hk}^{\rho}\right) \tag{B.12}.$$

We now take the energy equation, and we explicitate the two terms forming the total energy:

$$A_h\left(\frac{\partial \rho_h i_h}{\partial t} + \frac{\partial \rho_h v_h^2/2}{\partial t}\right) + \left(\frac{\partial \rho_h V_h i_h}{\partial x} + \frac{\partial \rho_h V_h v_h^2/2}{\partial x}\right) + \frac{\partial p_h V_h}{\partial x} = -\sum_{k=1}^{H}\left(1-\delta_{hk}\right)\Gamma_{hk}^{e} + \dot{q}_h' + \dot{q}_{cf,h}' \tag{B.13}$$

and we subtract the continuity equation multiplied by $i_h+v_h^2/2$, to obtain:

$$A_h\rho_h\frac{\partial i_h}{\partial t} + \rho_h V_h \frac{\partial i_h}{\partial x} + p_h \frac{\partial V_h}{\partial x} + v_h \underline{\underline{\left(\rho_h \frac{\partial V_h}{\partial t} + \frac{\rho_h V_h}{A_h}\frac{\partial V_h}{\partial x} + A_h \frac{\partial p_h}{\partial x} - \frac{\rho_h V_h^2}{A_h^2}\frac{\partial A_h}{\partial x}\right)}} = \tag{B.14}$$

$$-\sum_{k=1}^{H}\left(1-\delta_{hk}\right)\left[\Gamma_{hk}^{e} - \left(i_h + \frac{v_h^2}{2}\right)\Gamma_{hk}^{\rho}\right] + \dot{q}_h' + \dot{q}_{cf,h}'$$

that has been already grouped conveniently. The term underlined can be further reduced using the momentum balance (B.12), obtaining:

$$A_h\rho_h\frac{\partial i_h}{\partial t} + \rho_h V_h \frac{\partial i_h}{\partial x} + p_h \frac{\partial V_h}{\partial x} = V_h F_h - \sum_{k=1}^{H}\left(1-\delta_{hk}\right)\left[\Gamma_{hk}^{e} - v_h\Gamma_{hk}^{v} - \left(i_h - \frac{v_h^2}{2}\right)\Gamma_{hk}^{\rho}\right] + \dot{q}_h' + \dot{q}_{cf,h}' \tag{B.15}.$$

We can now use the relation (B.8) to substitute for the di_h differentials in Eq. (B.15), and we obtain:

$$A_h \rho_h C_h \frac{\partial T_h}{\partial t} + \rho_h V_h C_h \frac{\partial T_h}{\partial x} + \frac{p_h}{\rho_h}\underline{\underline{\left(A_h \frac{\partial \rho_h}{\partial t} + \frac{\partial \rho_h V_h}{\partial x} \right)}} - \varphi_h C_h T_h \underline{\underline{\left(A_h \frac{\partial \rho_h}{\partial t} + V_h \frac{\partial \rho_h}{\partial x} \right)}} =$$
$$= V_h F_h - \sum_{k=1}^{H} \left(1 - \delta_{hk}\right) \left[\Gamma_{hk}^{e} - v_h \Gamma_{hk}^{v} - \left(i_h - \frac{v_h^2}{2} \right) \Gamma_{hk}^{\rho} \right] + \dot{q}'_h + \dot{q}'_{cf,h} \tag{B.16}$$

that can be reduced using the continuity equation (B.5) to substitute the terms underlined and to obtain the desired energy balance in non-conservative form:

$$A_h \rho_h C_h \frac{\partial T_h}{\partial t} + \rho_h V_h C_h \frac{\partial T_h}{\partial x} + \rho_h \varphi_h C_h T_h \frac{\partial V_h}{\partial x} =$$
$$V_h F_h - \sum_{k=1}^{H} \left(1 - \delta_{hk}\right) \left[\Gamma_{hk}^{e} - v_h \Gamma_{hk}^{v} - \left(h_h - \frac{v_h^2}{2} - \varphi_h C_h T_h \right) \Gamma_{hk}^{\rho} \right] + \dot{q}'_h + \dot{q}'_{cf,h} \tag{B.17}$$

A third equation is needed, the non-conservative form of the continuity balance. This is obtained substituting the $d\rho_h$ differenmtial using the thermodynamic identity (B.9) in the continuity equation (B.5):

$$A_h \frac{\partial p_h}{\partial t} + V_h \frac{\partial p_h}{\partial x} + \rho_h c_h^2 \frac{\partial V_h}{\partial x} + \rho_h c_h^2 v_h \frac{\partial A_h}{\partial x} - \varphi_h \underline{\underline{\left(A_h \rho_h \frac{\partial i_h}{\partial t} - \rho_h V_h \frac{\partial i_h}{\partial x} - p_h \frac{\partial V_h}{\partial x} \right)}}$$
$$- \sum_{k=1}^{H} \left(1 - \delta_{hk}\right) \left(c_h^2 - \frac{p_h \varphi_h}{\rho_h} \right) \Gamma_{hk}^{\rho} \tag{B18}.$$

We reduce further the equation above, in particular the terms underlined, adding the non-conservative intermediate form of the energy equation Eq. (B.15) multiplied by φ_h, and we obtain:

$$A_h \frac{\partial p_h}{\partial t} + V_h \frac{\partial p_h}{\partial x} + \rho_h c_h^2 \frac{\partial V_h}{\partial x} =$$
$$- \sum_{k=1}^{H} \left(1 - \delta_{hk}\right) \left\{ c_h^2 \Gamma_{hk}^{\rho} + \varphi_h \left[\Gamma_{hk}^{e} - v_h \Gamma_{hk}^{v} - \left(h_h - \frac{v_h^2}{2} \right) \Gamma_{hk}^{\rho} \right] \right\} + \varphi_h V_h F_h + \varphi_h \dot{q}'_h + \varphi_h \dot{q}'_{cf,h} \tag{B.19}.$$

that is the desired non-conservative continuity balance.

11 Derivation of the Electric Model

To derive the equations that govern the diffusion of current in a cable formed by E parallel electrically conductive we start examining the current and voltages on an elemental length dx. Figure C.1 schows schematically this length for the particular case of 3 electric components. Over this length the generic component e has longitudinal resistance $R_e=r_e\,dx$, where r_e is the resistance per unit length (zero if the component is in superconducting state). The E components have self inductance $L_{e,e}$ and are inductively coupled through mutual inductances $L_{e,f}$. For reason of convenience in the following derivation we write the inductances on a unit length basis as $L_{e,f}=l_{e,f}\,dx$. It must be noted here that, unlike the case of longitudinal resistance, the inductance coefficients per unit length are not independent on dx and care should be taken in their use, as we will discuss later. Finally each component can have an external voltage source $V^{ext}_e=v^{ext}_e\,dx$ that can be originated, for instance, by changes of the magnetic flux linked with the component.

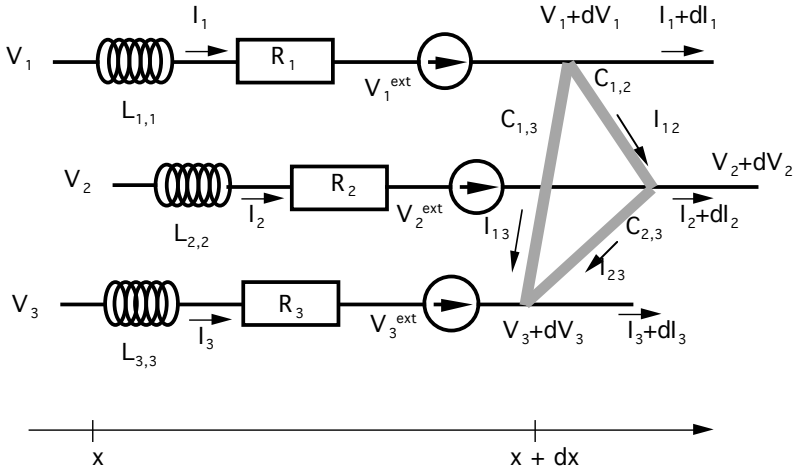

Figure C.1. Element dx of a three strand circuit used to demonstrate the derivation of the electric model. It is assumed that the structure represented repeats along the cable length with period dx.

The generic component has a current I_e and voltage V_e at the coordinate x. Over the elemental length dx the current will change by dI_e because of the current transfer through the transverse resistances with all other components $R_{e,f}$ = 1 / $C_{e,f}$ where $C_{e,f}$ is the transverse conductance among components e and f. As for other quantities we define $C_{e,f}$ on a unit length basis as $c_{e,f}\,dx$ introducing the the transverse conductance per unit length $c_{e,f}$.

The voltage will change over the length dx by $d\,V_e$ because of the parallel resistance, inductance and the voltage source along the component. We can write the following equation for the voltage of component e along the elemental mesh identified (Kirchhoff Voltage Law):

$$V_e - r_e I_e dx - \sum_{f=1}^{E} \int_{-x}^{L-x} l_{e,f}(x, x-\xi) \frac{\partial I_f(x-\xi)}{\partial t} d\xi + v_e^{ext} dx = V_e + dV_e \tag{C.1}$$

where the integral term gives the inductive contribution from the total cable length L and expresses the fact that in principle the whole cable length will contribute through inductive coupling to the equations for the element dx located at x along the cable. We assume for simplicity that the coupling is weak for all sections, except for the length dx located at x, and we obtain the following simpler expression:

$$V_e - r_e I_e dx - \sum_{f=1}^{E} l_{e,f} \frac{\partial I_f}{\partial t} dx + v_e^{ext} dx = V_e + dV_e \tag{C.2}$$

which is *local* to the elemental length examined. From Eq. (C.2) we can write the following differential equation for each of the E components:

$$-r_e I_e - \sum_{f=1}^{E} l_{e,f} \frac{\partial I_f}{\partial t} + v_e^{ext} = \frac{\partial V_e}{\partial x} \tag{C.3}$$

that provides the balance for the voltage change along each component. It is however more convenient to combine all equations introducing voltage differences with respect to a single component that we take as reference. The choice of the reference is arbitrary, and we choose to take the last component. Equation (C.3) gives origin to the following set of E-1 equations involving the E currents in the components:

$$-r_e I_e + r_E I_E - \sum_{f=1}^{E} \left(l_{e,f} - l_{E,f}\right) \frac{\partial I_f}{\partial t} + v_e^{ext} - v_E^{ext} = \frac{\partial \left(V_e - V_E\right)}{\partial x} \tag{C.4}$$

where we note that in the inductive term the inductance coefficients appear only as differences. At this point we remark that while the inductance of a single line depends on the line length, and diverges as the length goes to infinite, the differences appearing in Eq. (C.4) have a finite limit for infinite length.

The voltage relations above must be complemented by equations for the current conservation in the system. The current balance in each component is written (Kirchhoff Current Law):

$$I_e = \sum_{\substack{f=1 \\ f \neq e}}^{E} I_{ef} + I_e + dI_e \tag{C.5}.$$

where we have introduced the transverse current I_{ef} between components e and f . A suitable expression for the current transfer among two components can be written using the transverse conductance as follows:

$$I_{ef} = C_{e,f}\left(V_e - V_f\right) = c_{e,f}\,dx\left(V_e - V_f\right) \tag{C.6}$$

and using Eq. (C.6) to substitute in Eq. (C.5) we obtain:

$$dI_e = -\sum_{\substack{f=1 \\ f\neq e}}^{E} c_{e,f}\,dx\left(V_e - V_f\right) \tag{C.7}.$$

Once more it is more convenient to write the above current balance taking one component (e.g. component E) as voltage reference and arranging terms to have only the E-1 voltage differences with respect to this component:

$$dI_e = c_{e,1}dx\left(V_1 - V_E\right) + c_{e,2}dx\left(V_2 - V_E\right) + \ldots - \sum_{\substack{f=1 \\ f\neq e}}^{E} c_{e,f}\,dx\left(V_e - V_E\right) + \ldots + c_{e,E-1}dx\left(V_{E-1} - V_E\right) \tag{C.8}.$$

From the above balance we obtain finally the following E differential equation for the variation of the current in all components:

$$\frac{\partial I_e}{\partial x} = c_{e,1}\left(V_1 - V_E\right) + c_{e,2}\left(V_2 - V_E\right) + \ldots - \sum_{\substack{f=1 \\ f\neq e}}^{E} c_{e,f}\left(V_e - V_E\right) + \ldots + c_{e,E-1}\left(V_{E-1} - V_E\right) \tag{C.9}.$$

In the absence of current sinks and sources, which is the case in a cable, the total current in the cable I_{total} is constant along the whole cable length. Therefore at any position$x$ the single currents in the components must satisfy the condition:

$$\sum_{e=1}^{E} I_e = I_{total} \tag{C.10}.$$

The condition Eq. (C.10) implies in addition that:

$$\sum_{e=1}^{E} \frac{\partial I_e}{\partial x} = 0 \tag{C.11}.$$

Note that the condition Eq. (C.11) can be obtained adding all the E equations of the system of Eqs. (C.9). This means also that using the condition Eq. (C.10) automatically reduces the rank of the system of Eqs. (C.9).

We wish now to eliminate the voltage differences from the system of Eqs. (C.4) and (C.9). To ease further algebra we write Eqs. (C.4), (C.9) and (C.10) in matrix notation as follows:

$$-\tilde{\mathbf{r}}\mathbf{I} - \tilde{\mathbf{l}}\frac{\partial \mathbf{I}}{\partial t} + \Delta\tilde{\mathbf{v}}^{ext} = \frac{\partial \Delta \mathbf{V}}{\partial x} \tag{C.12}$$

$$\frac{\partial \tilde{\mathbf{I}}}{\partial x} = -\tilde{\mathbf{c}}\Delta\mathbf{V} \tag{C.13}.$$

$$\mathbf{bI} = I_{total} \tag{C.14}.$$

where we have defined the following vectors and matrices:

$$\Delta\mathbf{V} = \begin{bmatrix} V_1 - V_E \\ V_2 - V_E \\ \vdots \\ V_e - V_E \\ \vdots \\ V_{E-1} - V_E \end{bmatrix} \tag{C.15}$$

$$\mathbf{I} = \begin{bmatrix} I_1 \\ I_2 \\ \vdots \\ I_e \\ \vdots \\ I_E \end{bmatrix} \tag{C.16}$$

$$\Delta\tilde{\mathbf{v}}^{ext} = \begin{bmatrix} v_1^{ext} - v_E^{ext} \\ v_2^{ext} - v_E^{ext} \\ \vdots \\ v_e^{ext} - v_E^{ext} \\ \vdots \\ v_{E-1}^{ext} - v_E^{ext} \end{bmatrix} \tag{C.17}$$

$$\tilde{\mathbf{r}} = \begin{bmatrix} r_1 & 0 & \cdots & 0 & \cdots & 0 & -r_E \\ 0 & r_2 & \cdots & 0 & \cdots & 0 & -r_E \\ & & \ddots & & & & \\ 0 & 0 & 0 & r_e & \cdots & 0 & -r_E \\ & & & & \ddots & & \\ 0 & 0 & \cdots & & \cdots & r_{E-1} & -r_E \end{bmatrix} \tag{C.18}$$

$$\tilde{\mathbf{l}} = \begin{bmatrix} l_{1,1}-l_{1,E} & l_{1,2}-l_{2,E} & \cdots & l_{1,e}-l_{e,E} & \cdots & l_{1,E-1}-l_{E-1,E} & l_{1,E}-l_{E,E} \\ l_{2,1}-l_{1,E} & l_{2,2}-l_{2,E} & \cdots & l_{2,e}-l_{e,E} & \cdots & l_{2,E-1}-l_{E-1,E} & l_{2,E}-l_{E,E} \\ & & \ddots & & & & \\ l_{e,1}-l_{1,E} & l_{e,2}-l_{2,E} & \cdots & l_{e,e}-l_{e,E} & \cdots & l_{e,E-1}-l_{E-1,E} & l_{e,E}-l_{E,E} \\ & & & & \ddots & & \\ l_{E-1,1}-l_{1,E} & l_{E-1,1}-l_{1,E} & \cdots & & \cdots & l_{E-1,E-1}-l_{E-1,E} & l_{E-1,E}-l_{E,E} \end{bmatrix} \tag{C.19}$$

$$\hat{\mathbf{c}} = \begin{bmatrix} \sum_{\substack{f=1 \\ f\neq 1}}^{E} c_{1,f} & -c_{1,2} & \cdots & -c_{1,e} & \cdots & -c_{1,E-1} \\ -c_{1,2} & \sum_{\substack{f=1 \\ f\neq 2}}^{E} c_{2,f} & \cdots & -c_{2,e} & \cdots & -c_{2,E-1} \\ & & \ddots & & & \\ -c_{e,1} & -c_{e,2} & \cdots & \sum_{\substack{f=1 \\ f\neq e}}^{E} c_{e,f} & \cdots & -c_{e,E-1} \\ & & & & \ddots & \\ -c_{E-1,1} & -c_{E-1,2} & \cdots & -c_{E-1,e} & \cdots & \sum_{\substack{f=1 \\ f\neq E-1}}^{E} c_{E-1,f} \end{bmatrix} \tag{C.20}$$

$$\mathbf{b} = \begin{bmatrix} 1 & 1 & \cdots & 1 & \cdots & 1 & 1 \end{bmatrix} \tag{C.21}.$$

The vector $\tilde{\mathbf{I}}$ is obtained from the vector **I** removing the last row. If the inverse of the matrix $\tilde{\mathbf{c}}$ exists (this is always the case for finite values of the conductivity), it is possible to take the space derivative of Eq. (C.13) as follows:

$$\frac{\partial}{\partial x}\left(\tilde{\mathbf{c}}^{-1}\frac{\partial \tilde{\mathbf{I}}}{\partial x}\right) = -\frac{\partial \Delta \mathbf{V}}{\partial x} \tag{C.22}$$

and substitute in Eq. (C.12) leading to the following system of *E*-1 equations for the *E* currents:

$$\tilde{\mathbf{l}}\frac{\partial \mathbf{I}}{\partial t} + \tilde{\mathbf{r}}\mathbf{I} - \frac{\partial}{\partial x}\left(\tilde{\mathbf{c}}^{-1}\frac{\partial \tilde{\mathbf{I}}}{\partial x}\right) = \Delta \tilde{\mathbf{v}}^{ext} \tag{C.23}.$$

We complement the system above with the condition on the total current, Eq. (C.14), and we finally obtain the desired system:

$$\mathbf{l}\frac{\partial \mathbf{I}}{\partial t} + \mathbf{r}\mathbf{I} - \frac{\partial}{\partial x}\left(\mathbf{c}^{-1}\frac{\partial \mathbf{I}}{\partial x}\right) = \Delta \mathbf{v}^{ext} \qquad \text{(C.24)}.$$

where the matrices and vectors in Eq. (C.24) have been obtained by block assembly of the matrices and vectors defined previously:

$$\Delta \mathbf{v}^{ext} = \begin{bmatrix} \Delta \widetilde{\mathbf{v}}^{ext} \\ I_{total} \end{bmatrix} \qquad \text{(C.25)}$$

$$\mathbf{l} = \begin{bmatrix} \widetilde{\mathbf{l}} \\ \mathbf{0} \end{bmatrix} \qquad \text{(C.26)}$$

$$\mathbf{r} = \begin{bmatrix} \widetilde{\mathbf{r}} \\ \mathbf{b} \end{bmatrix} \qquad \text{(C.27)}$$

$$\mathbf{c}^{-1} = \begin{bmatrix} \widetilde{\mathbf{c}}^{-1} & \mathbf{0} \\ \mathbf{0} & 0 \end{bmatrix} \qquad \text{(C.28)}$$

and the symbol **0** indicates zero filling.

12 Boundary Conditions for Electric Model

The system of Eqs. (C.24) is a parabolic PDE for the currents in the strands and requires therefore two boundary conditions. In analogy with a diffusion problems, we define two types of boundary conditions: given current at the boundary (Dirichlet condition) and given voltage (Von Neumann condition). To clarify the meaning of the two conditions we can imagine that the cable is spread at the ends as shown in Fig. D.1. The current boundary condition corresponds to placing a current generator in series with each component. The current flowing at the boundary in component e is then given simply by:

$$I_e = I_{boundary} \tag{D.1}$$

where $I_{boundary}$ is the current flowing in the current generator attached to the component.

The voltage boundary condition corresponds to placing a voltage generator at the boundary between the components e and E, the last component among those defined. This follows from the definition of the voltage difference in Eq. (C.8). The voltage generator at the boundary adds to the external voltage difference. In particular for any component e the voltage difference at the boundary node is given by:

$$\Delta\tilde{v}^{ext} = v_e^{ext} - v_E^{ext} + \Delta v_{boundary} \tag{D.2}$$

where $\Delta v_{boundary}$ is the voltage from the boundary voltage generator. This modifies the entries in the vector of voltage differences defined in Eq. (C.17) and Eq. (C.25). Note finally that using the voltage boundary condition and setting $\Delta v_{boundary}$=0 we can model the case of shorted electric components at the boundary.

The boundary conditions of the two types described above can be set independently on each other on both boundaries, i.e. voltage condition on one boundary and current condition on the other boundary or different current conditions on the two boundaries. In addition they can be mixed for different components on the same boundary, i.e. a current condition on one component and a voltage condition on another one on the same boundary. They are however mutually exclusive, i.e. the imposition of a current boundary condition on one component prevents the simultaneous imposition of a voltage boundary condition on the same component. In addition, as we have stated in Appendix C, the total current in the cable must satisfy Eq. (C.10) at any position along the cable length, therefore also at the boundary. This implies that the number of independent boundary conditions that can be applied to a set of E electric components is E-1, and the missing boundary condition is implied by

the use of Eq. (C.10) in the system Eq. (C.24). This is consistent with the structure of the system of PDE, where we have assembled E-1 differential equations and one integral condition.

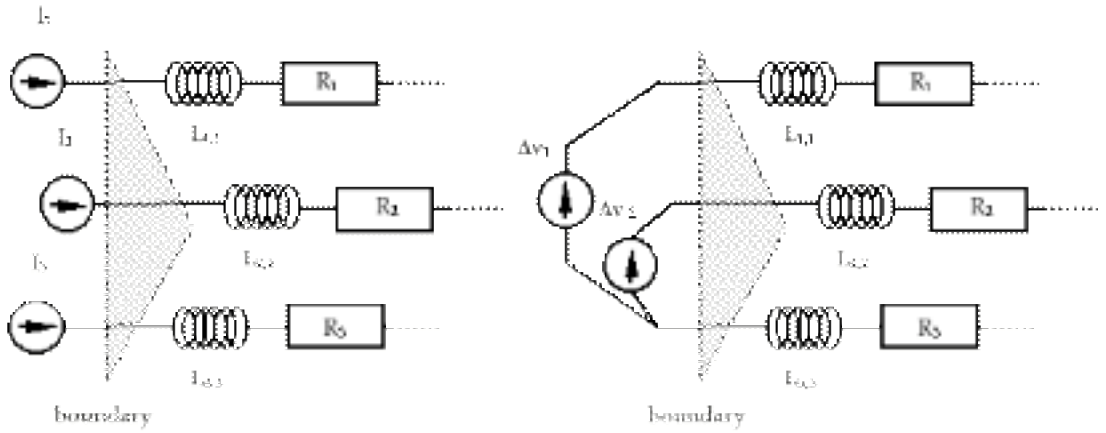

Figure D.1 Principle of application of boundary conditions to an assembly of electric components. Dirichlet conditions (left) correspond to a current generator in series with each component, Von Neumann conditions (right) correspond to a voltage generator between each component and the last component.

13 Joule Power Dissipated by Transverse Current Transfer Among Electric Components

The current transfer that takes place between components through the transverse conductance is necessarily associated with Joule heat generation. The heat generated by currents flowing in superconducting components and closing across the transverse resistances in a cable is generally referred to as AC losses. Although the order of magnitude of AC losses is small compared to Joule heating in a strand above current sharing, its contribution to the temperature increase and eventually the transition of a superconductor can be significant. It is therefore important to quantify it. We compute first the heat generated in each transverse conductance. To do this we start calculating the voltage differences among each component and the reference component. From Eq. (C.13) we have that:

$$\Delta\mathbf{V} = -\tilde{\mathbf{c}}^{-1}\frac{\partial\tilde{\mathbf{I}}}{\partial x} \tag{E.1}$$

where the derivative of the currents along the length of the cable is supposed to be known from the solution of the electric problem. Once the vector $\Delta\mathbf{V}$ is known, it is possible to compute the voltage difference $\Delta V_{e,f}$ between each couple of components e and f as follows:

$$\Delta V_{e,f} = V_e - V_f = (V_e - V_E) - (V_f - V_E) = \Delta V_e - \Delta V_f \tag{E.2}$$

where ΔV_e and ΔV_f are the entries e and f in the vector $\Delta\mathbf{V}$. The power generated per unit length by the current flowing between components e and f is then given by:

$$\dot{q}'_{e,f} = c_{e,f}\Delta V_{e,f}^2 \tag{E.3}.$$

We now make the simplified assumption that this power is equally distributed among the two components. The total power in each component can be obtained adding all contributions as follows:

$$\dot{q}'_{transverse,e} = \sum_{\substack{f=1 \\ f\neq e}}^{E}\frac{1}{2}\dot{q}'_{e,f} \tag{E.4}.$$

14 Adaptive Meshing

Mesh adaptivity is the key to achieving accurate solution avoiding the unnecessary memory and computation time overhead associated with the use of a uniform, fine mesh. We have implemented an *h*-adaptivity algorithm that consists of three steps. The first step is the generation of an ideal mesh density profile that satisfies specified error criteria, where the mesh density d is defined as the inverse of the element size Δx, or:

$$d = \frac{1}{\Delta x} \qquad \text{(F.1).}$$

The density profile is defined on the existing (*old*) mesh. In the second step a *new* mesh is generated in accordance with the desired mesh density profile. Finally, in the third step, the variables are interpolated from the *old* mesh to the *new* mesh.

The new mesh generated consists of elements of the same type (number of nodes and interpolation order). We therefore do not perform *p*-adaptivity (variable order elements), which would add a considerable complication in mesh generation and book-keeping.

14.1 Mesh Density

The mesh density is defined so that all elements have a size Δx in the interval $[\Delta x_{min} \ldots \Delta x_{max}]$, where the minimum and maximum element sizes are specified by the user. We have considered three possible criteria to define the ideal mesh density, as given below.

14.1.1 User's specified refined region.

The region has a given center $x_{refined}$ and a refined mesh length $L_{refined}$. The mesh density profile for this case is shown schematically in Fig. F.1. The region $L_{refined}$ centered around $x_{refined}$ has a uniform mesh density d_{max} (corresponding to the minimum element size Δx_{min}). Outside this region the mesh density decreases gradually to the minimum d_{min} (corresponding to the minimum element size Δx_{max}). We can write the density profile as follows:

$$d(x) = \max\left\{ d_{\min} + d_{\max} W(x, x_{\min}, x_{\max}), d_{\max} e^{-[d_{\max}(x - x_{\min})]^2}; d_{\max} e^{-[d_{\max}(x - x_{\max})]^2} \right\} \qquad \text{(F.1).}$$

where the function $W(x,x_{min},x_{max})$ is a window which has value 1 between x_{min} and x_{max}, and 0 outside. The two boundaries of the window are the beginning and end of the refined region:

$$x_{\min} = x_{refined} - \frac{L_{refined}}{2} \tag{F.2}$$

$$x_{\max} = x_{refined} + \frac{L_{refined}}{2} \tag{F.3}.$$

The exponential functions are built to achieve a transition from the minimum element size in the refined region to the maximum element size in the outside region over a sufficient number of elements.

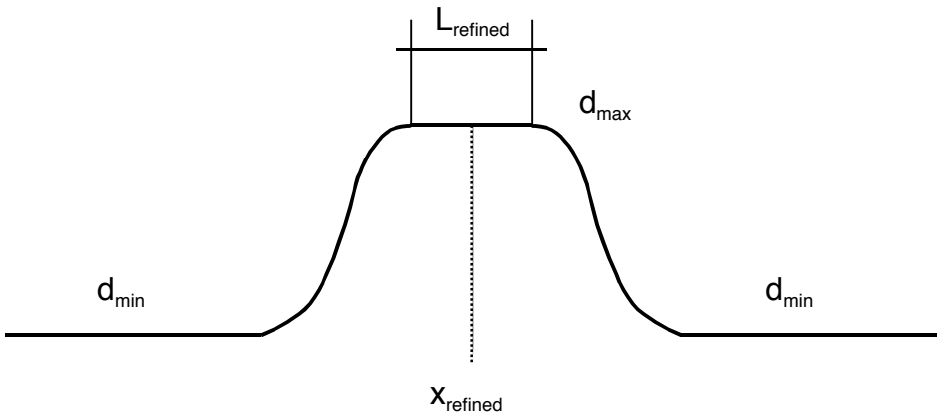

Figure F.1 Density profile in the case of a user's refined region centered at $x_{refined}$ and with length $L_{refined}$. The profile in the transition region outside the refinement is a gaussian.

14.1.2 Tracking of physical discontinuities and propagating fronts

Physical discontinuities and propagating fronts can be the lambda transition region from normal to superfluid helium, or the transition from superconducting to normal conducting state at the fronts of the normal zone in a quenching superconducting cable. The front is located at the position x_{front}. The mesh density profile for this case is shown schematically in Fig. F.2, and has the following equation:

$$d(x) = \max\left\{ d_{\min}; d_{\max} e^{-\left[d_{\max}\left(x - x_{front}\right)\right]} \right\} \tag{F.4}.$$

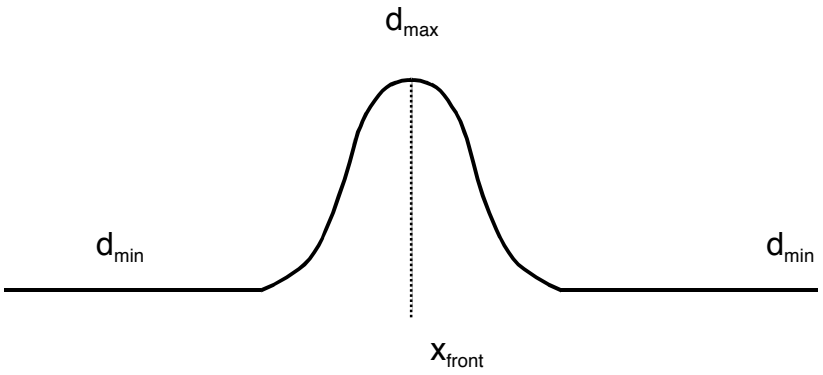

Figure F.2 Density profile in the case of a front centered at x_{front}. The profile around the front is a gaussian.

14.1.3 Interpolation error

A final way to determine the mesh density profile is to estimate the interpolation error in the solution. The principle in this case is to estimate the error on an element-by-element basis and to define a mesh density that would make the interpolation error uniform throughout the complete mesh. To estimate the interpolation error we recall that for an element of order n any function $u(x)$ is interpolated with an error of order $O(\Delta x^{n+1})$ given locally by:

$$e = c\Delta x^{n+1}\left|\frac{\partial^{n+1}u}{\partial x^{n+1}}\right| \tag{F.5}$$

where c is an arbitrary constant. Taking for simplicity c = 1, and setting a maximum *reasonable* interpolation error e_{max} for the mesh, the requirement that $e = e_{max}$ can be written in terms of the desired mesh density as follows:

$$d = \frac{1}{\Delta x}\sqrt[n+1]{\frac{e}{e_{\max}}} \tag{F.6}.$$

The difficulty in this process is in the evaluation of the derivative in Eq. (F.5). A possible method is to evaluate the first derivative of the variable u(x) using the shape functions in the element (see Appendix G) and the nodal values U:

$$\frac{\partial u}{\partial x} \approx \frac{1}{J}\frac{\partial N}{\partial \xi}U \tag{F.7}$$

The jacobian of the element J is defined as:

$$J = \frac{\partial x}{\partial \xi} \approx \frac{\partial N}{\partial \xi} x \qquad \text{(F.8).}$$

Note that if the internal nodes are equally spaced the Jacobian is constant in the element. The first order derivative is evaluated at the nodes in the mesh, and we denote it with $\frac{\partial U}{\partial x}$. $\frac{\partial U}{\partial x}$ is discontinuous at the boundary among elements, i.e. it has a left and a right value. We produce a smoothed, single valued distribution $\frac{\partial U^*}{\partial x}$ averaging the nodal values at the inter-element boundaries. We finally recover the derivative of order n+1 by using again the shape function derivatives:

$$\frac{\partial^{n+1} u}{\partial x^{n+1}} \approx \left(\frac{1}{J}\right)^{n+1} \frac{\partial^n N}{\partial \xi^n} \frac{\partial U^*}{\partial x} \qquad \text{(F.9)}$$

where we have made use of the fact J is constant. Because the derivatives of order n of the shape functions are non-zero and constant (see Appendix G), the value obtained for $\frac{\partial^{n+1} u}{\partial x^{n+1}}$ is a constant in the element, and can be use to estimate the interpolation error.

In the case of a vector function **u**(x) the above procedure can be applied either to a control component (e.g. temperature) or to all components of the vector. The result is a set of mesh density distribution whose upper envelope is the desired mesh density.

14.2 Mesh Generation

The mesh is generated based on the upper envelope of the mesh density profiles defined using the methods described above. To do this we first compute the integrated density function $D(x)$ defined as:

$$D(x) = \int_0^x d(x')\,dx' \qquad \text{(F.10).}$$

This function has the property that $D(L)$ is the total number of elements to be generated. The extremes of the elements are placed using the inverse mapping $x(D)$, subdividing the D interval in $D(L)$ equispaced elements. The nodes within an element are placed so that they are equispaced in x, thus avoiding possible problems with the finite element Jacobian in the case of non-uniform mapping

of coordinates. This procedure achieves quickly and without iteration the desired mesh density.

14.3 Variable Interpolation

The final step is to interpolate variables from the old mesh to the new mesh. For consistency reasons the interpolation is performed using the finite element representation of the variables. For the interpolation of a vector variable $\mathbf{U}^{old}$ at any point x it is firstly necessary to determine the normalised position of the point ξ_x in the parent element. This is a straightforward matter for elements with uniformly spaced internal nodes:

$$\xi_x = 2\frac{x - x_1}{\Delta x} - 1 \tag{F.11}$$

where x_1 is the coordinates of the first node of the element, and Δx is its size. Once the normalised position in the element is known, the interpolation is performed using the shape functions:

$$\mathbf{U}^{new} \approx \mathbf{N}(\xi_x)\mathbf{U}^{old} \tag{F.12}.$$

15 Finite Element Shape Functions

The finite element discretization in space requires the definition of shape functions N and of their derivatives dN/dx. We report here the shape functions and derivatives for a 1-D Lagrangian element with interpolation order from linear to quintic. The finite element is defined in the *parent space* as shown in Fig. G-1. The local coordinate ξ is centered in the element and spans the interval [-1…+1]. The tables G-1 through G-5 report the location of the nodes in the parent space for lagrangian elements of order 1 to 5, the shape functions N(ξ) and their first derivative dN/dξ (i.e. with respect to ξ). Finally we also report the last non-zero derivative of the shape functions, $d^nN/d\xi^n$, useful for the calculation of the interpolation error in an element.

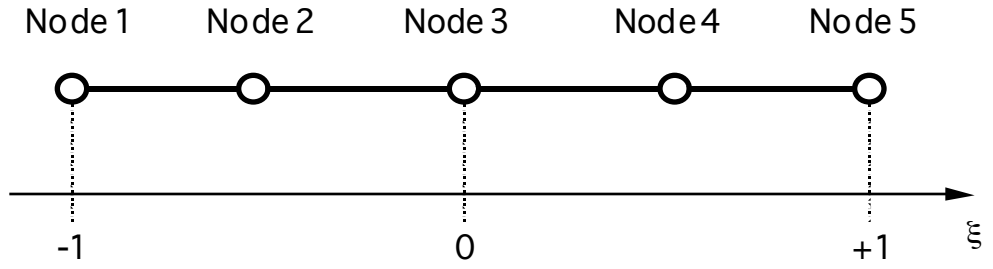

Figure G-1. Definition of a finite element (5 nodes) and its local coordinate ξ in the parent plane.

Table G-1. Linear element.

node	ξ	N	dN/dξ	$d^nN/d\xi^n$
1	-1	$\frac{1-\xi}{2}$	$-\frac{1}{2}$	-1/2
2	1	$\frac{1+\xi}{2}$	$\frac{1}{2}$	1/2

Table G-2. Quadratic element.

node	ξ	N	dN/dξ	$d^nN/d\xi^n$
1	-1	$\frac{\xi(\xi-1)}{2}$	$\xi-\frac{1}{2}$	1
2	0	$1-\xi^2$	-2ξ	-2
3	1	$\frac{\xi(\xi+1)}{2}$	$\xi+\frac{1}{2}$	1

Table G-3. Cubic element.

node	ξ	N	dN/dξ	$d^nN/d\xi^n$
1	-1	$-\frac{9}{16}\left(\xi^2-\frac{1}{9}\right)(\xi-1)$	$-\frac{9}{16}\left(3\xi^2-2\xi-\frac{1}{9}\right)$	-27/8
2	-1/3	$\frac{27}{16}\left(\xi^2-1\right)\left(\xi-\frac{1}{3}\right)$	$\frac{27}{16}\left(3\xi^2-\frac{2}{3}\xi-1\right)$	81/8
3	1/3	$-\frac{27}{16}\left(\xi^2-1\right)\left(\xi+\frac{1}{3}\right)$	$-\frac{27}{16}\left(3\xi^2+\frac{2}{3}\xi-1\right)$	-81/8
4	1	$\frac{9}{16}\left(\xi^2-\frac{1}{9}\right)(\xi+1)$	$\frac{9}{16}\left(3\xi^2+2\xi-\frac{1}{9}\right)$	27/8

Table G-4. Quartic element.

node	ξ	N	dN/dξ	$d^nN/d\xi^n$
1	-1	$\frac{2}{3}\xi\left(\xi^2-\frac{1}{4}\right)(\xi-1)$	$\frac{2}{3}\left(4\xi^3-3\xi^2-\frac{1}{2}\xi+\frac{1}{4}\right)$	16
2	-1/2	$-\frac{8}{3}\xi\left(\xi^2-1\right)\left(\xi-\frac{1}{2}\right)$	$-\frac{8}{3}\left(4\xi^3-\frac{3}{2}\xi^2-2\xi+\frac{1}{2}\right)$	-64
3	0	$4\left(\xi^2-\frac{1}{4}\right)\left(\xi^2-1\right)$	$4\left(4\xi^3-\frac{5}{2}\xi\right)$	96
4	1/2	$-\frac{8}{3}\xi\left(\xi^2-1\right)\left(\xi+\frac{1}{2}\right)$	$-\frac{8}{3}\left(4\xi^3+\frac{3}{2}\xi^2-2\xi-\frac{1}{2}\right)$	-64
5	1	$\frac{2}{3}\xi\left(\xi^2-\frac{1}{4}\right)(\xi+1)$	$\frac{2}{3}\left(4\xi^3+3\xi^2-\frac{1}{2}\xi-\frac{1}{4}\right)$	16

Table G-5. Quintic element.

node	ξ	N	dN/dξ	$d^nN/d\xi^n$
1	-1	$-\frac{625}{768}\left(\xi^2-\frac{9}{25}\right)\left(\xi^2-\frac{1}{25}\right)(\xi-1)$	$-\frac{625}{768}\left(5\xi^4-4\xi^3-\frac{30}{25}\xi^2+\frac{20}{25}\xi+\frac{9}{625}\right)$	-3125/32
2	-3/5	$\frac{3125}{768}\left(\xi^2-1\right)\left(\xi^2-\frac{1}{25}\right)\left(\xi-\frac{3}{5}\right)$	$\frac{3125}{768}\left(5\xi^4-\frac{12}{5}\xi^3-\frac{78}{25}\xi^2+\frac{156}{125}\xi+\frac{1}{25}\right)$	15625/32
3	-1/5	$\frac{3125}{384}\left(\xi^2-1\right)\left(\xi^2-\frac{9}{25}\right)\left(\xi-\frac{1}{5}\right)$	$\frac{3125}{384}\left(5\xi^4-\frac{4}{5}\xi^3-\frac{102}{25}\xi^2-\frac{68}{125}\xi+\frac{9}{25}\right)$	15625/16
4	1/5	$-\frac{3125}{384}\left(\xi^2-1\right)\left(\xi^2-\frac{9}{25}\right)\left(\xi+\frac{1}{5}\right)$	$-\frac{3125}{384}\left(5\xi^4+\frac{4}{5}\xi^3-\frac{102}{25}\xi^2+\frac{68}{125}\xi+\frac{9}{25}\right)$	-15625/16
5	3/5	$-\frac{3125}{768}\left(\xi^2-1\right)\left(\xi^2-\frac{1}{25}\right)\left(\xi+\frac{3}{5}\right)$	$-\frac{3125}{768}\left(5\xi^4+\frac{12}{5}\xi^3-\frac{78}{25}\xi^2-\frac{156}{125}\xi+\frac{1}{25}\right)$	-15625/32
6	1	$\frac{625}{768}\left(\xi^2-\frac{9}{25}\right)\left(\xi^2-\frac{1}{25}\right)(\xi+1)$	$\frac{625}{768}\left(5\xi^4+4\xi^3-\frac{30}{25}\xi^2-\frac{20}{25}\xi+\frac{9}{625}\right)$	3125/32

16 Gauss Integration

The matrices in Eqs. (7.3) through (7.6) and the vector Eq. (7.7) need numerical evaluation as the arguments of the integrals are notnecessarily known or integrable analytical functions. To perform the integration we resort on the local character of the shape functions over the finite elements. Any integral over the complete domain of integration can be obtained by assembly of integrals over the single elements. Integration over each element is in turn obtained using the Gauss rule, which offers the best compromise between the number of points he evaluation of the integrand and the accuracy of the result. We take as a general example the integral of the function *f(x)* over an element of length Δx:

$$F = \int_{\Delta x} f(x)dx \tag{H.1}$$

The function *f(x)* can be a vector function of the coordinate x, as indeed is the case for Eqs. (7.3) through (7.7). In this case the integration is intended to be performed on each component of the vector. We can write the integral Eq. (H.1) in an alternative form that makes use of the coordinate transformation between a finite element in the physical and in the parent space:

$$F = \int_{-1}^{1} f(x(\xi))\frac{dx}{d\xi}d\xi \tag{H.2}$$

where ξ is the normalised coordinate in the parent space (see Appendix G). The derivative $dx/d\xi$ is also called the Jacobian J of the transformation. We can now apply the Gauss integration method to the integral above:

$$F \approx \sum_{g=1}^{Ng} W_g J(\xi_g) f(x(\xi_g)) \tag{H.3}$$

where we note that the integral has been approximated by a sum of N_g terms. The terms of the sum consist of the integrand evaluated at the Gauss points ξ_g, weighted by the Gauss weights W_g. The coordinates of the Gauss points and the values of the Gauss weights depend only on the total number of points (i.e. the *rule*) used, and are found tabulated as shown in Tab. H1.

It is a known property of Gauss integration that the method described above can integrate exactly a polynomial of order 2 N_g-1. Therefore depending on the order of the integrand it is possible to fix the number of Gauss points to be used. In our case we use systematically a number of Gauss points $N_g = n + 1$ where n is the order of the shape function of the element. This choice

guarantees that the integrals in Eqs. (7.3) to (7.7) do not give origin to singular matrices.

Table H-1. Gauss point coordinates and Gauss weights for the integration rules implemented.

$\pm\xi_g$	W_g
N_g=1	
0.000 000 000 000 000	2.000 000 000 000 000
N_g=2	
0.577 350 269 189 626	1.000 000 000 000 000
N_g=3	
0.774 596 669 241 483	0.555 555 555 555 556
0.000 000 000 000 000	0.888 888 888 888 889
N_g=4	
0.861 136 311 594 953	0.347 854 845 137 454
0.339 981 043 584 856	0.652 145 154 862 546
N_g=5	
0.906 179 845 938 664	0.236 926 885 056 189
0.538 469 310 105 683	0.478 628 670 499 366
0.000 000 000 000 000	0.568 888 888 888 889
N_g=6	
0.932 469 514 203 152	0.171 324 492 379 170
0.661 209 386 466 265	0.360 761 573 048 139
0.238 619 186 083 197	0.467 913 934 572 691